ORGANOMETALLICS

ARTICLE

pubs.acs.org/Organometallics

Influences of N-Heterocyclic Carbene and PMe_3 Ligands on the Tautomerism between Methylene/Hydride and Bridging Methyl Complexes of Rh/Os and Unusual Examples of Ligand Deprotonation by the NHC Group

Kyle D. Wells,[†] Robert McDonald,[‡] Michael J. Ferguson,[‡] and Martin Cowie*[,†]

[†]Department of Chemistry and [‡]X-ray Crystallography Laboratory, University of Alberta, Edmonton, Alberta, Canada T6G 2G2

Supporting Information

ABSTRACT:

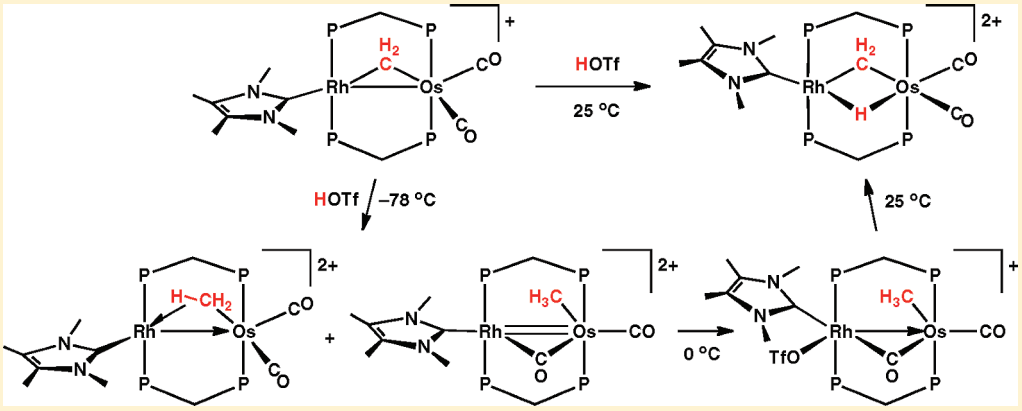

The complexes $[RhOsL(CO)_3(dppm)_2][CF_3SO_3]$ (L = IMe_4 (1,3,4,5-tetramethylimidazol-2-ylidene) (**6**), PMe_3 (**8**); dppm = μ-$Ph_2PCH_2PPh_2$) were prepared by substitution of a carbonyl ligand in $[RhOs(CO)_4(dppm)_2][CF_3SO_3]$. Reaction of **6** with additional IMe_4 resulted in deprotonation of a dppm ligand, yielding $[RhOs(IMe_4)(CO)_3(\mu\text{-}\kappa^1\text{:}\kappa^1\text{-}Ph_2PCHPPh_2)(dppm)]$ (**7**). Although reaction of **8** with diazomethane at −78 °C yielded the known methylene-bridged $[RhOs(PMe_3)(CO)_3(\mu\text{-}CH_2)(dppm)_2][CF_3SO_3]$ (**3**), compound **6** was unreactive toward diazomethane over a wide temperature range. The methylene-bridged species $[RhOs(IMe_4)(CO)_2(\mu\text{-}CH_2)(dppm)_2][CF_3SO_3]$ (**9**) was obtained by reaction of $[RhOs(CO)_3(\mu\text{-}CH_2)(dppm)_2][CF_3SO_3]$ with IMe_4, although $[RhOs(CO)_3(\mu\text{-}CH_2)(\mu\text{-}\kappa^1\text{:}\eta^2\text{-}Ph_2PCHPPh_2)(dppm)]$ (**10**) was also obtained by competing dppm deprotonation by IMe_4. Protonation of $[RhOsL(CO)_2(\mu\text{-}CH_2)(dppm)_2][CF_3SO_3]$ (L = IMe_4 (**9**), PMe_3 (**11**)) with triflic acid at −78 °C yielded two isomers in each case. The more abundant isomer, $[RhOsL(CO)_2(\mu\text{-}CH_3)(dppm)_2][CF_3SO_3]_2$, has a bridging agostic methyl group, while the minor isomer has a terminal, Os-bound methyl group. Upon warming, both isomers transformed to species having an Os-bound methyl group and a coordinated triflate ion, subsequently rearranging to the thermodynamic products $[RhOsL(CO)_2(\mu\text{-}H)(\mu\text{-}CH_2)(dppm)_2][CF_3SO_3]_2$ near ambient temperature. Attempts to prepare an IMe_4-containing methyl species directly via triflate ion substitution in $[RhOs(CH_3)(OSO_2CF_3)(CO)_3(dppm)_2][CF_3SO_3]$ by IMe_4 instead resulted in deprotonation of the methyl group to give the known product $[RhOs(CO)_3(\mu\text{-}CH_2)(dppm)_2][CF_3SO_3]$. Addition of methyl triflate to **6** gave no reaction, but protonation of **6** with triflic acid at −78 °C yielded the kinetic isomer of $[RhOsH(IMe_4)(CO)_3(dppm)_2][CF_3SO_3]_2$, in which the hydride is terminally bound to Os, and warming this product to ambient temperature resulted in rearrangement to the hydride-bridged, thermodynamic isomer.

INTRODUCTION

Bridging methyl groups can play an important role in a number of chemical transformations such as alkyl transfers,[1] carbon−hydrogen bond activation,[1c,2] and olefin polymerization.[3] The most common arrangement for methyl groups that bridge a pair of late metals is the unsymmetric bridging mode,[4] shown as structure **A** in Chart 1, in which the methyl ligand is σ-bound through carbon to one metal while also being involved in an agostic interaction with an adjacent metal. The potential involvement of such a structure in the facile C−H bond activation of surface-bound methyl groups[5] is obvious, particularly for late metals for which α-hydrogen elimination at a single metal is not common. Such facile C−H bond activation of methyl groups, presumably through an intermediate such as **A**, has

Received: October 22, 2010
Published: April 20, 2011

Chart 1

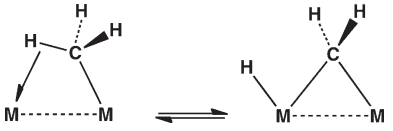

been observed in late-metal clusters,[2b,4a,6] which can serve as valuable models for related surface-promoted transformations.[7]

A common approach for generating unsymmetrically bridged methyl groups is by protonation of methylene-bridged precursors,[4d,e,8,9] although in some cases the favored product is instead the methylene/hydride tautomer (**B**)[2b,6c,10] and not a species containing an intact methyl group. Shapley and co-workers have demonstrated that the equilibrium between tautomers **A** and **B** in a triosmium cluster could be shifted toward the methylene-bridged hydride species (**B**) through substitution of a carbonyl ligand by a more basic phosphine ligand.[11]

We have previously investigated the protonation reactions of a series of methylene-bridged complexes $[MM'(CO)_4(\mu\text{-}CH_2)(dppm)_2]^+$ (M = Rh, M′ = Ru,[8b] Os;[8a] M = Ir, M′ = Ru[8d]) and have found in all cases that the apparent kinetic product is an unsymmetrically bridged methyl species, which is stable only at low temperature, converting upon slight warming to a product containing a conventional, terminally bound methyl group on the group 9 metal. Unlike the case for the Shapley study,[11] substituting a carbonyl in the Rh/Os system by a number of different phosphine ligands did not yield the methylene/hydride products, although this substitution did stabilize the unsymmetrically bridged methyl group, allowing these products to be isolated at ambient temperature.[8c]

On the basis of the well-documented analogies between phosphine and N-heterocyclic carbene (NHC) ligands,[12,13] we sought to extend the above studies on the $[RhOsL(CO)_3(\mu\text{-}CH_2)(dppm)_2]^+$ systems (L = CO, PR_3) by substituting L by the NHC ligand 1,3,4,5-tetramethylimidazol-2-ylidene (IMe_4), in order to determine if the superior donor strength of IMe_4 would favor the methylene/hydride species (**B**), in which the metals can be considered to be in a higher formal oxidation state than in the agostic methyl tautomer (**A**). In this paper our attempts to compare the effects of the IMe_4 and PMe_3 ligands on the methyl/methylene hydride tautomerism, shown in Chart 1, are reported, together with some unanticipated reactivity involving the NHC ligand.

EXPERIMENTAL SECTION

General Comments. All solvents were dried using the appropriate desiccants, distilled before use, and stored under nitrogen. Reactions were performed under an argon atmosphere using standard Schlenk techniques. The 1,3,4,5-tetramethylimidazol-2-ylidene ligand (IMe_4) was prepared using a published procedure[14] and then recrystallized from toluene to afford colorless crystals, which were stored at −30 °C. For reactions that did not require its isolation, a standardized solution containing IMe_4 in THF (0.2133 M) was stored over potassium metal in the freezer and used without further purification.

The compounds $[RhOs(CO)_4(dppm)_2][CF_3SO_3]$ (**1**),[15] $[RhOs(CO)_3(\mu\text{-}CH_2)(dppm)_2][CF_3SO_3]$ (**2**),[16] $[RhOs(PMe_3)(CO)_3(\mu\text{-}CH_2)(dppm)_2][CF_3SO_3]$ (**3**),[8c] $[RhOs(CO)_4(\mu\text{-}CH_2)(dppm)_2][CF_3SO_3]$ (**4**),[16] and $[RhOs(Me)(OSO_2CF_3)(CO)_3(dppm)_2][CF_3SO_3]$ (**5**)[8c] were prepared using their respective published procedures, and the labeled $^{13}CH_2$ and ^{13}CO analogues were prepared by substituting Diazald-*N*-methyl-^{13}C or ^{13}CO in the preparations.

All reagents were purchased from Sigma-Aldrich, unless otherwise noted, and used as is. $[H(OEt_2)_2][BAr^F{}_4]$ ($BAr^F{}_4 = B(3,5\text{-}(CF_3)_2C_6H_3)_4$) was prepared according to the published procedure.[17] PMe_3 (1 M solution in THF) and neat triflic acid (CF_3SO_3H = HOTf) were transferred into Teflon-capped Schlenk flasks and stored in the refrigerator under argon. Diazomethane was generated in situ from a methanolic slurry containing Diazald, by the slow dropwise addition of KOH(aq) (5.3 M). The generated gas was transferred directly via cannula to the reaction flask without further drying. Carbon monoxide was purchased from Praxair, and the ^{13}CO (99%) was obtained from Cambridge Isotope Laboratories.

The NMR spectra were recorded using a Varian iNova-400 spectrometer operating at 399.8 MHz for ^1H, 161.8 MHz for ^{31}P, and 100.6 MHz for ^{13}C nuclei. Infrared spectra were obtained on solutions using a Nicolet Magna 760 spectrometer or on solid samples using a NicPlan FTIR spectrometer. Elemental analyses were performed by the microanalytical service within the department using a CE 1108 CHNS-O analyzer. Electrospray ionization mass spectra (EIMS) were acquired on a Micromass ZabSpec spectrometer by the staff in the departmental mass spectrometry laboratory. In all cases the distribution of isotopic peaks matched the calculated distribution for the appropriate parent ion very closely. Spectroscopic data for all compounds are given in Table 1.

Preparation of Compounds. *(a). $[RhOs(IMe_4)(CO)_3(dppm)_2][CF_3SO_3]$ (**6**).* One equivalent of IMe_4 (0.71 mL, 0.2133 M THF) was added via syringe to a solution containing compound **1** (200 mg, 0.15 mmol) in 10 mL of THF. After the mixture was stirred for 30 min, Et_2O (25 mL) was added to precipitate the product. The resulting yellow solid (200 mg, 94%) was dried in vacuo. HRMS: *m/z* calcd for $C_{60}H_{56}N_2O_3P_4RhOs$ ($M^+ - CF_3SO_3$) 1271.1911, found 1271.1918 ($M^+ - CF_3SO_3$). Anal. Calcd for $C_{61}H_{56}N_2F_3O_6P_4RhOsS$: C, 51.62; H, 3.98; N, 1.97. Found: C, 51.23; H, 4.06; N, 2.23.

*(b). $[RhOs(IMe_4)(CO)_3(Ph_2PCHPPh_2)(dppm)]$ (**7**)*

Method i. Excess IMe_4 (1.78 mL, 0.2133 M THF, 2.5 equiv) was added via cannula to **1** (200 mg, 0.15 mmol) dissolved in 15 mL of THF. After 30 min, the resulting orange solution was concentrated to an oily residue before 5 mL of pentane was added, giving a bright yellow solid (approximately 74%). This procedure led to contamination of the product by the resulting $[HIMe_4][OTf]$ salt, which remained in an approximate 1:10 ratio with the product. To purify the product, a concentrated dichloromethane solution containing the crude solid was layered with pentane, affording platelike crystals of **7** overnight (60 mg, 28%).

Method ii. The addition of IMe_4 (0.20 mL, 2.133×10^{-1} M THF, 0.043 mmol) to compound **6** (50 mg, 0.04 mmol), dissolved in 3 mL of CH_3CN, instantly yielded a yellow precipitate from the resulting orange solution. This proved to be a more favorable route for the synthesis of **7**, since both the imidazolium salt and any remaining free carbene remained soluble in the mother liquor, allowing the solid sample to be readily separated. The resulting solid was isolated and further rinsed with 2×1 mL of CH_3CN before drying in vacuo (yield 84%). Anal. Calcd for $C_{60}H_{55}N_2O_3P_4RhOs \cdot 1.5CH_2Cl_2$: C, 52.89; H, 4.19; N, 2.01. Found: C, 52.85; H, 4.40; N, 2.06.

*(c). $[RhOs(PMe_3)(CO)_3(dppm)_2][CF_3SO_3]$ (**8**).* To a stirred solution containing **1** (100 mg, 0.076 mmol) in 10 mL of THF was added 80 μL of 1 M PMe_3 (0.08 mmol, THF solution), resulting in the darkening of the light yellow solution. A 20 mL portion of Et_2O was used to precipitate a yellow solid, which was rinsed with a further 10 mL portion of pentane before being allowed to dry in vacuo (yield 94 mg, 90%). HRMS: *m/z* calcd for $C_{56}H_{53}O_3P_5RhOs$ ($M^+ - CF_3SO_3$) 1223.1347, found 1223.1346 ($M^+ - CF_3SO_3$). Anal. Calcd for $C_{57}H_{53}F_3O_6P_5RhOsS$: C, 49.93; H, 3.90. Found: C, 49.52; H, 3.84.

*(d). $[RhOs(PMe_3)(CO)_3(\mu\text{-}CH_2)(dppm)_2][CF_3SO_3]$ (**3**).* Compound **8** (100 mg, 0.073 mmol) was dissolved in 15 mL of dichloromethane and

Table 1. Spectroscopic Data for the Compounds

compd	IR[a,b]	NMR[c]		
		$\delta(^{31}P\{^1H\})$[g]	$\delta(^1H)$[h,i]	$\delta(^{13}C\{^1H\})$[i]
$[RhOs(IMe_4)(CO)_3(dppm)_2][OTf]$ (**6**)	1967 (s), 1914 (s), 1785 (m)	29.4 (dm, $^1J_{PRh}$ = 132), −3.5 (m, dppm)[d]	3.58 (tt, 4H, $^2J_{HP(Os)}$, $^2J_{HP(Rh)}$ = 4.3, dppm); 2.71 (s, 6H, NCH_3), 1.61 (s, 6H, CCH_3, IMe_4)[d]	216.2 (dt, 2C, $^1J_{CRh}$ = 10, $^2J_{CP(Os)}$ = 9, μ-CO); 183.7 (t, 1C, $^2J_{CP(Os)}$ = 12, Os−CO); 176.4 (dt, 1C, $^1J_{CRh}$ = 50, $^2J_{CP(Rh)}$ = 16, C_{car}), 127.6 (s, 2C, C═C), 34.9 (s, 2C, NCH_3), 8.9 (s, 2C, CCH_3, IMe_4); 33.9 (tt, 2C, $^1J_{CP}$ = 15, 10, dppm)[d]
$[RhOs(IMe_4)(CO)_3(dppm\text{-}H)(dppm)]$ (**7**)	1960 (s), 1906 (s), 1744 (m)	P_A, 34.2 (dddd); P_B, −6.2 (ddd, dppm-H); P_C, 29.9 (dddd); P_D, −4.6 (ddd, dppm)[e] (J: P_AP_C, 345; P_AP_D, 44; P_AP_B, 145; P_CP_D, 87; P_BP_C, 43; P_BP_D, 188; P_ARh, 123; P_CRh, 130)	3.26 (dd, 2H, $^2J_{HP(Os)}$, $^2J_{HP(Rh)}$ = 8.7, dppm); 2.51 (bm, 1H, dppm-H); 2.65 (s, 6H, NCH_3), 1.00 (s, 6H, CCH_3, IMe_4)[e]	218.2 (ddd, 2C, $^1J_{CRh}$ = 7, $^2J_{CP(Os)}$ = 9, 9, μ-CO); 188.1 (dd, 1C, $^2J_{CP(Os)}$ = 13, 13, Os−CO); 38.0 (m, 1C, dppm-H); 35.2 (dd, 1C, $^1J_{CP}$ = 21, 16, dppm); 185.3 (ddd, 1C, $^1J_{CRh}$ = 52, $^2J_{CP}$ = 13, 13, C_{car}), 34.3 (s, 2C, NCH_3), 8.4 (s, 2C, CCH_3, IMe_4)[e]
$[RhOs(PMe_3)(CO)_3(dppm)_2][OTf]$ (**8**)	1987 (s), 1933 (s), 1771 (m)	28.7 (ddm, $^1J_{PRh}$ = 134, $^2J_{PP}$ = 40), −3.3 (m, dppm); −23.3 (dt, $^1J_{PRh}$ = 144, $^2J_{PP}$ = 40, PMe_3)[d]	4.11 (tt, 4H, $^2J_{HP(Os)}$, $^2J_{HP(Rh)}$ = 4.2, dppm); 0.16 (d, 9H, $^2J_{HP}$ = 8.4, PMe_3)[d]	209.9 (dt, 2C, $^1J_{CRh}$, $^2J_{CP(Os)}$ = 11, μ-CO); 182.5 (t, 1C, $^2J_{CP(Os)}$ = 14, Os−CO); 47.2 (m, 2C, dppm); 18.8 (d, 3C, $^1J_{CP}$ = 26, PMe_3)[d]
$[RhOs(IMe_4)(CO)_2(\mu\text{-}CH_2)\text{-}(dppm)_2][OTf]$ (**9**)	2031 (s), 1960 (m), 1936 (s)	25.0 (dm, $^1J_{PRh}$ = 132), −2.66 (m, dppm)[f]	8.71 (dtt, 2H, $^3J_{HP(Os)}$ = 15.4, $^3J_{HP(Rh)}$ = 5.5, $^1J_{CH}$ = 135.3, μ-CH_2); 4.55, 3.97 (m, 2H, $^2J_{HH}$ = 14.9, dppm); 3.14, 2.90, 2.63, 1.47 (s, 3H, IMe_4)[f]	188.5 (dt, 1C, $^2J_{CP(Os)}$ = 4, $^2J_{CC}$ = 11), 184.3 (t, 1C, $^2J_{CP(Os)}$ = 11, Os−CO); 179.7 (dt, 1C, $^1J_{CRh}$ = 48, $^2J_{CP}$ = 16, C_{car}), 34.6, 33.7, 8.2, 8.1 (s, 1C, CH_3, IMe_4); 121.3 (ddm, 1C, $^2J_{CRh}$ = 19, $^2J_{CC}$ = 11, μ-CH_2); 27.9 (m, 2C, dppm)[f]
$[RhOs(CO)_3(\mu\text{-}CH_2)(dppm\text{-}H)\text{-}(dppm)]$ (**10**)	1974 (s), 1956 (s), 1893 (s)	P_A, 48.5 (dddd); P_B, 6.5 (dd, dppm); P_C, −3.2 (ddd); P_D, −7.2 (dddd, dppm-H)[f] (J: P_AP_B, 89; P_AP_C, 18; P_AP_D, 2; P_BP_D, 282; P_CP_D, 21; P_ARh, 143; P_CRh, 87; P_DRh, 11)	5.18, 4.45 (dm, 1H, $^2J_{HH}$ = 6, $^1J_{CH}$ =134.5, μ-CH_2); 4.62 (ddd, 1H, $^2J_{HH}$ = 14, $^2J_{HP}$ = 23.4), 3.47 (bdd, 1H, $^2J_{HH}$ = 14.0, $^2J_{HP}$ = 23.4, dppm); 1.38 (m, 1H, $^2J_{HRh}$ = 1.6, dppm-H)[f]	188.2 (dm, 1C, $^1J_{CRh}$ = 65, Rh−CO); 188.1 (dd, 1C, $^2J_{CP(Os)}$ = 8, 8), 186.1 (dd, 1C, $^2J_{CP(Os)}$ = 7, 7, Os−CO); 75.0 (m, 1C, μ-CH_2, $^1J_{CRh}$ = 21); 40.0 (dd, 1C, $^1J_{CP}$ = 25, 25, dppm); 13.7 (m, 1C, dppm-H)[f]

dx.doi.org/10.1021/om1010066 |*Organometallics* 2011, 30, 2654–2669

Table 1. Continued

compd	IR[a,b]	NMR[c] $\delta(^{31}P\{^1H\})$[g]	NMR[c] $\delta(^1H)$[h,i]	NMR[c] $\delta(^{13}C\{^1H\})$[i]
$[RhOs(PMe_3)(\mu\text{-}CH_2)(CO)_2(dppm)_2][OTf]$ (**11**)	1982 (s), 1936 (m), 1894 (s)	25.7 (ddm, $^1J_{PRh}$ = 130, $^2J_{PP}$ = 38), 2.02 (m, dppm); −24.4 (dt, $^1J_{PRh}$ = 122, $^2J_{PP}$ = 38, PMe_3)[d]	7.09 (dtt, 2H, $^2J_{HP(Os)}$ = 14.5, $^2J_{HP(Rh)}$ = 7.2, $^2J_{HRh}$ = 2.6, μ-CH_2); 4.17 (dtt, 2H, $^2J_{HP(Os)}$, $^2J_{HP(Rh)}$ = 5.3, $^2J_{HH}$ = 14.9, dppm), 3.75 (ddtt, 2H, $^2J_{HP(Os)}$, $^2J_{HP(Rh)}$ = 3.6, $^2J_{HRh}$ = 2.4, $^2J_{HH}$ = 14.9, dppm); 0.31 (d, 9H, $^2J_{HP}$ = 7.5, PMe_3)[d]	187.3 (t, 1C, $^2J_{CC}$ = 12, $^2J_{CP(Os)}$ = 5), 180.2 (t, 1C, $^2J_{CP(Os)}$ = 10, Os−CO); 105.7 (dddtt, 1C, $^1J_{CH}$ = 133, $^2J_{CRh}$ = 17, $^2J_{CC}$ = 12, $^2J_{CP(Os)}$, $^2J_{CP(Rh)}$ = 5, μ-CH_2); 32.5 (m, 2C, dppm); 17.4 (d, 3C, $^1J_{CP}$ = 23, PMe_3)[d]
$[RhOs(IMe_4)(CO)_2(\mu\text{-}CH_3)(dppm)_2][OTf]_2$ (**12a**)	NA	20.2 (dm, $^1J_{PRh}$ = 118), −1.9 (m, dppm)[d,j]	4.34, 3.70 (dm, 2H, $^2J_{HH}$ = 14.7, dppm); 4.00, 2.41, 2.02, 1.10 (s, 3H, IMe_4); 0.08 (brd, 3H, $^1J_{CH}$ = 111, CH_3)[d,j]	183.4 (brdt, 1C, $^2J_{CC}$ = 11, $^2J_{CP(Os)}$ = 5), 169.6 (t, 1C, $^2J_{CP(Os)}$ = 8, Os−CO); 7.9 (brq, 1C, $^1J_{CH}$ = 111, μ-CH_3)[d,j]
$[RhOs(IMe_4)(CH_3)(CO)_2(dppm)_2]$-$[OTf]_2$ (**12b**)	NA	14.2 (dm, $^1J_{PRh}$ = 118), −11.7 (m, dppm)[d,j]	1.60 (brd, $^1J_{CH}$ = 125, HMQC required)[d,j]	203.6 (dt, 1C, $^1J_{CRh}$ = 23, μ-CO); 178.8 (t, 1C, $^2J_{CP(Os)}$ = 7, CO); −28.8 (q, 1C, $^1J_{CH}$ = 125, CH_3)[d,j]
$[RhOs(PMe_3)(CO)_2(\mu\text{-}CH_3)(dppm)_2][OTf]_2$ (**13a**)	NA	15.9 (ddm, $^1J_{PRh}$ = 156, $^2J_{PP}$ = 37), −4.0 (m, dppm); 8.3 (ddt, $^1J_{PRh}$ = 162, $^2J_{PP}$ = 37, $^3J_{PC}$ = 12, PMe_3)[d,j]	4.62, 3.29 (brm, 2H, dppm); 0.76 (d, 9H, $^2J_{HP}$ = 7.4, PMe_3); −0.74 (brd, $^1J_{CH}$ = 117, μ-CH_3)[d,j]	182.0 (dt, 1C, $^2J_{CC}$ = 12, $^2J_{CP}$ = 5), 169.0 (t, 1C, $^2J_{CP}$ = 7, CO); −6.0 (qd, 1C, $^1J_{CH}$ = 117, $^1J_{CC}$ = 12, μ-CH_3)[d,j]
$[RhOs(PMe_3)(CH_3)(CO)_2(dppm)_2]$-$[OTf]_2$ (**13b**)	NA	19.6 (ddm, $^1J_{PRh}$ = 116, $^2J_{PP}$ = 38), 0 (brm, dppm); −18.3 (ddt, $^1J_{PRh}$ = 160, $^2J_{PP}$ = 38, $^3J_{PC}$ = 34, PMe_3)[d,j]	3.88, 3.68 (brdm, 2H, $^2J_{HH}$ = 13.1, dppm); 0.93 (brd, $^1J_{CH}$ = 126, HMQC required); 0.81 (d, 9H, $^2J_{HP}$ = 7.4, PMe_3)[d,j]	193.6 (dt, 1C, $^1J_{CRh}$ = 18, $^2J_{CP(Os)}$ = 7, μ-CO); 179.5 (dt, 1C, $^2J_{CP(Os)}$, $^2J_{CC}$ = 10 Hz, Os−CO); −29.2 (qdd, 1C, $^1J_{CH}$ = 126, $^2J_{CP}$ = 34, $^2J_{CC}$ = 10, CH_3)[d,j]
$[RhOs(CH_3)(OTf)(IMe_4)(\mu\text{-}CO)(CO)(dppm)_2][OTf]$ (**14**)	NA	14.9 (dm, $^1J_{PRh}$ = 126 Hz), 9.00 (m, dppm)[d,l]	4.95, 3.56 (dtt, 2H, $^2J_{HH}$ = 13.2, $^2J_{HP(Os)}$, $^2J_{HP(Rh)}$ = 5.5, dppm); 4.10, 1.97, 1.96, 1.25 (s, 3H, IMe_4); 0.18 (dt, 3H, $^1J_{CH}$ = 133.0, $^3J_{HP}$ = 6.3)[d,l]	205.9 (ddt, 1C, $^1J_{CRh}$ = 39, $^2J_{CP}$ = 8, $^2J_{CC}$ = 6, μ-CO), 177.6 (dt, 1C, $^2J_{CP}$ = 9, $^2J_{CC}$ = 4, Os−CO); 13.8 (qd, 1C, $^1J_{CH}$ = 133.0, $^2J_{CC}$ = 6, CH_3)[d,l]
$[RhOs(CH_3)(OTf)(PMe_3)(\mu\text{-}CO)$-$(CO)(dppm)_2][OTf]$ (**15**)	NA	18.9 (ddm, $^1J_{PRh}$ = 121, $^2J_{PP}$ = 40), 6.8 (m, dppm); −12.0 (ddt, $^1J_{PRh}$ = 163, $^2J_{PP}$ = 40, $^3J_{PC}$ = 40, PMe_3)[d,k]	4.15, 3.82 (dm, 2H, $^2J_{HH}$ = 13, dppm); 0.57 (d, 9H, $^2J_{HP}$ = 9.9, PMe_3); 0.06 (dt, 3H, $^1J_{CH}$ = 132.7, $^3J_{HP}$ = 6.8)[d,k]	199.5 (ddd, 1C, $^1J_{CRh}$ = 40, $^2J_{CP}$ = 40, $^2J_{CC}$ = 7, μ-CO); 176.3 (dt, 1C, $^2J_{CP}$ = 10, $^2J_{CC}$ = 4, Os−CO); 14.5 (qd, 1C, $^1J_{CH}$ = 133.0, $^2J_{CC}$ = 7, CH_3)[d,k]

dx.doi.org/10.1021/om1010066 |*Organometallics* 2011, 30, 2654–2669

Table 1. Continued

compd	IR[a,b]	NMR[c] $\delta(^{31}P\{^1H\})$[g]	NMR[c] $\delta(^1H)$[h,i]	NMR[c] $\delta(^{13}C\{^1H\})$[i]
$[RhOs(IMe_4)(CO)_2(\mu\text{-}CH_2)(\mu\text{-}H)(dppm)_2][OTf]_2$ (**16**)	NA	17.9 (dm, $^1J_{PRh}$ = 113), −12.1 (m, dppm)[d]	4.54, 3.25 (dtt, 2H, $^2J_{HH}$ = 15.5, $^2J_{HP(Os)}$, $^2J_{HP(Rh)}$ = 5.2); 6.63 (dtt, 2H, $^1J_{CH}$ = 133.7, $^3J_{HP(Os)}$, $^3J_{HP(Rh)}$ = 8.5, μ-CH_2); 3.05, 3.03, 2.60, 2.23 (s, 3H, IMe_4); −11.47 (dm, 1H, $^1J_{RhH}$ = 14.8, μ-H)[d]	179.2 (t, 1C, $^2J_{CC}$ = 14, $^2J_{CP}$ = 8), 173.2 (t, 1C, $^2J_{CP}$ = $^2J_{CH}$ = 7, Os−CO); 99.6 (tdm, 1C, $^1J_{CH}$ = 133, $^1J_{CRh}$ = 32, μ-CH_2)[d]
$[RhOs(PMe_3)(CO)_2(\mu\text{-}CH_2)(\mu\text{-}H)(dppm)_2][OTf]_2$ (**17**)	NA	15.0 (ddm, $^1J_{PRh}$ = 103, $^2J_{PP}$ = 36), −13.3 (m, dppm); −18.8 (dt, $^1J_{PRh}$ = 139, $^2J_{PP}$ = 36, PMe_3)[d]	4.02 (brm, 4H, dppm); 6.22 (dtt, 2H, $^1J_{CH}$ = 138.7, $^3J_{HP(Os)}$, $^3J_{HP(Rh)}$ = 6.0, μ-CH_2); 1.02 (d, 9H, $^2J_{HP}$ = 9.8, PMe_3); −10.90 (ddm, 1H, $^1J_{RhH}$ = 15.0, $^2J_{HP}$ = 60.0, μ-H)[d]	176.7 (dt, $^2J_{CC}$ = 14, $^2J_{CP}$ = 5), 176.4 (dt, 1C, $^2J_{CP}$ = 10, $^2J_{CH}$ = 7, Os−CO); 79.4 (tdm, 1C, $^1J_{CH}$ = 139, $^1J_{CRh}$ = 36, $^2J_{CC}$ = 15, μ-CH_2)[d]
$[RhOs(CH_3)(PMe_3)(OEt_2)(CO)_2(dppm)_2][BPh_4][BAr^F{}_4]$ (**18**)	2049 (s), 1998 (s)	P_A, 60.2 (dddd); P_B, −4.6 (dd); P_C, −11.5 (ddd); P_D, −44.1 (ddd); P_E, −60.4 (dd) (*J*: P_AP_B, 46; P_AP_C, 15; P_AP_D, 14; P_CP_D, 219; P_CP_E, 29; P_DP_E, 31; P_ARh, 216; P_BRh, 189)[d]	5.55 (ddt, 1H, $^2J_{HP(Os)}$, $^2J_{HP(Rh)}$ = 10.3, $^4J_{HP}$ = 4.8, $^2J_{HH}$ = 16.0), 3.42 (dt, 1H, $^2J_{HP(Os)}$, $^2J_{HP(Rh)}$ = 8.2, $^2J_{HH}$ = 16.0, dppm); 4.97 (dt, 1H, $^2J_{HP(Os)}$, $^2J_{HP(Rh)}$ = 12.0, $^2J_{HH}$ = 17.3), 3.05 (dm, 1H, $^2J_{HH}$ = 17.3, dppm); 0.82 (d, 9H, $^2J_{HP}$ = 10.8, PMe_3); 0.48 (ddd, 3H, $^3J_{HP}$ = 7.4, CH_3);[j] 3.98 (q, 2H, $^3J_{HH}$ = 6.9), 1.33 (t, 3H, $^3J_{HH}$ = 6.9, OEt_2)[d]	178.3 (ddd, 1C, $^1J_{CRh}$ = 83, $^2J_{CP(Rh)}$ = 7, Rh−CO); 176.5 (ddd, 1C, $^2J_{CP}$ = 8, $^2J_{CP(Os)}$ = 8, μ-CO); 49.5 (dd, 1C, $^1J_{CP}$ = 24, 16, dppm); 44.0 (ddd, 1C, $^1J_{CP}$ = 36, 31, $^2J_{CRh}$ = 7, dppm); −20.5 (ddd, 1C, $^2J_{CP}$ = 8, Os−CH_3)[d]
$[RhOs(IMe_4)(CO)_3(H)(dppm)_2][OTf]_2$ (**19a**)	NA	22.7 (dm, $^1J_{RhP}$ = 111), −3.9 (m, dppm)[d,l]	3.65, 3.53 (brdm, 2H, $^2J_{HH}$ = 14.3, dppm); 2.94, 2.37, 1.77, 1.71 (s, 3H, CH_3, IMe_4); −5.94 (t, 1H, $^2J_{HP}$ = 15.6, H)[d,l]	211.4 (dm, 1C, $^1J_{CRh}$ = 24, $^2J_{CH}$ = 11, μ-CO); 198.6 (dt, 1C, $^1J_{CRh}$ = 18, $^2J_{CP}$ = 3.5), 173.8 (dt, 1C, $^2J_{CP(Os)}$ = 9, Os-CO); 161.7 (dt, 1C, $^1J_{CRh}$ = 63, $^2J_{CP}$ = 19, C_{car}), 35.3, 35.2 (s, 1C, NCH_3), 9.2, 8.9 (s, 1C, CCH_3, IMe_4); 26.7 (dd, 2C, $^1J_{CP}$ = 14, dppm)[d,l]
$[RhOs(IMe_4)(CO)_3(\mu\text{-}H)(dppm)_2][OTf]_2$ (**19b**)	2059 (s), 2011 (s), 1787 (s)	23.6 (dm, $^1J_{PRh}$ = 114), −8.7 (m, dppm)[d]	4.30 (dtt, 2H, $^2J_{HH}$ = 13.2, $^2J_{HP}$ = 4.9, 5.7), 3.79 (dtt, 2H, $^2J_{HH}$ = 13.2, $^2J_{HP(Os)}$, $^2J_{HP(Rh)}$ = 4.0, dppm); 3.32, 2.17, 1.65, 1.60 (s, 3H, IMe_4); −10.91 (dtt, 1H, $^1J_{RhH}$ = 18.8, $^2J_{HP}$ = 9.3, 7.3, μ-H)[d]	223.5 (dm, 1C, $^1J_{CRh}$ = 29, μ-CO); 176.7, 171.6 (t, 1C, $^2J_{CP}$ = 9, Os−CO); 161.9 (dt, 1C, $^1J_{CRh}$ = 57, $^2J_{CP}$ = 17, C_{car}), 36.0, 34.2 (s, 1C, NCH_3), 9.6, 8.4 (s, 1C, CCH_3, IMe_4); 29.9 (dd, 2C, $^1J_{CP}$ = 26, 14, dppm)[d]

[a] IR abbreviations: s = strong, m = medium, br = broad. [b] FTIR microscope; in units of cm^{-1}. [c] NMR abbreviations: br = broad, s = singlet, d = doublet, *t* = triplet, m = multiplet. NMR data at 298 K given in ppm (*J* values in Hz). [d] In CD_2Cl_2. [e] In C_6D_6. [f] In C_4D_8O. [g] ^{31}P chemical shifts referenced to external 85% H_3PO_4. [h] Chemical shifts for the phenyl hydrogens and carbons not given. [i] ^1H and ^{13}C chemical shifts referenced to TMS. [j] −80 °C. [k] −40 °C. [l] 0 °C.

dx.doi.org/10.1021/om1010066 |*Organometallics* 2011, 30, 2654–2669

the resulting solution cooled to −78 °C in a dry ice/acetone bath. Gaseous diazomethane (18 equiv), generated from 300 mg (1.4 mmol) of Diazald, was passed through the solution for 1 h. The solution was kept at −78 °C for another 1 h while being purged with argon gas. Once it was warmed to ambient temperature, the resulting solution was concentrated to approximately 5 mL in vacuo before 20 mL of Et_2O was used to precipitate the yellow solid (yield 94%). LRMS: *m*/*z* calcd for $C_{57}H_{55}O_3P_5RhOs$ ($M^+ - CF_3SO_3$) 1237.2, found 1237.2. ^1H, $^{13}C\{^1H\}$, and $^{31}P\{^1H\}$ NMR spectra of this product were identical with those of a previously characterized sample, prepared by another route.[8c]

*(e). [RhOs(IMe$_4$)(CO)$_2$(μ-CH$_2$)(dppm)$_2$][CF$_3$SO$_3$] (**9**) + [RhOs(CO)$_3$-(μ-CH$_2$)(Ph$_2$PCHPPh$_2$)(dppm)] (**10**).* A deep red solution containing compound **2** (300 mg, 0.23 mmol) in 5 mL of THF was cooled to −78 °C using a dry ice/acetone bath. A heavy argon purge was employed before 1.1 equiv of IMe_4 (1.2 mL, 0.213 M THF) was added dropwise via syringe. The resulting dark red solution was stirred for 2 h before being warmed to ambient temperature. An aliquot of the reaction mixture showed a 6:2:1 mixture of the desired product **9**, the deprotonated species **10** (vide supra), and the tetracarbonyl species $[RhOs(CO)_4(\mu\text{-}CH_2)(dppm)_2][OTf]$ (**4**) (formed from CO scavenging by **2**), respectively, as determined by ^{31}P NMR spectroscopy. Compounds **9** and **4**, along with $[HIMe_4][OTf]$, were precipitated as a dark red oil by the addition of 10 mL of pentane to the reaction mixture. The resulting bright yellow supernatant containing **10** was separated from the oil and evaporated to dryness in vacuo. The remaining crude product, containing **4** and **9**, was dissolved in a mixture of 4 mL of benzene and 1 mL of THF, leaving behind a yellow precipitate, determined by ^{31}P NMR spectroscopy to be compound **4**. The dark red supernatant was transferred to a new flask, and 10 mL of pentane was added to fully precipitate a dark oily solid which was rinsed with 5 mL of Et_2O and dried in vacuo, yielding approximately 40% of **9**. Failure to completely separate **9** from residual $[HIMe_4][OTf]$ gave unsatisfactory elemental analyses. NMR spectra for **9** are available as Supporting Information. HRMS: *m*/*z* calcd for $C_{60}H_{58}N_2O_2P_4RhOs$ ($M^+ - CF_3SO_3$) 1257.2113, found 1257.2112 ($M^+ - CF_3SO_3$).

*(f). Reaction of [RhOs(IMe$_4$)(CO)$_2$(μ-CH$_2$)(dppm)$_2$][CF$_3$SO$_3$] (**9**) with CO.* A dark red solution containing compound **9** (30 mg, 0.021 mmol) in 0.7 mL of C_6D_6 was gently purged with CO gas, causing the solution to immediately turn orange. After 5 min a yellow precipitate formed, which was separated from the mother liquor and dissolved in CD_2Cl_2. ^{31}P NMR spectroscopy (in CD_2Cl_2) established that the precipitate was **6**. When wet C_6D_6 was employed for the same procedure, the mother liquor showed the formation of acetic acid, as determined from ^{13}C and ^1H NMR spectroscopy.

*(g). [RhOs(PMe$_3$)(CO)$_2$(μ-CH$_2$)(dppm)$_2$][CF$_3$SO$_3$] (**11**).* A solution consisting of 50 mg (0.036 mmol) of **3** in 0.7 mL of CD_2Cl_2 was added to a NMR tube containing 6 equiv of trimethylamine oxide (TMNO; 16 mg, 0.22 mmol) via cannula with no immediate reaction. The solution was warmed to 39 °C in the NMR instrument and the reaction monitored to completion using ^{31}P NMR (taking approximately 30 min). Once the reaction was complete, the dark green solution was immediately cooled in a dry ice/acetone bath and 1 mL of pentane was added to precipitate a dark green oil. The yellow mother liquor left behind contained the suspected impurities, $[RhOsCl(CO)_2(\mu\text{-}CH_2)(dppm)_2]$ and $OPMe_3$, which were decanted to waste. A 1 mL portion of Et_2O was then employed to triturate the remaining oil. The light green ethereal solution was removed from the resulting dark green solid, which was dissolved in 0.2 mL of CH_2Cl_2 and then precipitated fully using a 1.5 mL portion of Et_2O, isolated, and allowed to dry further in vacuo (yield 77%). Anal. Calcd for $C_{57}H_{55}F_3O_5OsP_5RhS$: C, 50.45; H, 4.08; S, 2.36. Found: C, 50.38; H, 3.99; S, 2.22.

*(h). Protonation of Compounds **9** and **11** by HOTf at Ambient Temperature.* One equivalent of HOTf was added to a dark red solution of **9** (50 mg, 0.036 mmol) or a dark green solution of **11** (50 mg, 0.037 mmol) in 0.7 mL of CD_2Cl_2, causing each solution to immediately turn orange. In both cases the resulting solutions were stirred for 1 h and then 1 mL of pentane was added to fully precipitate yellow solids containing the respective products $[RhOs(L)(CO)_2(\mu\text{-}CH_2)(\mu\text{-}H)(dppm)_2][CF_3SO_3]_2$ (L = IMe_4 (**16**), PMe_3 (**17**)), which were dried in vacuo. Data for **16**: HRMS *m*/*z* calcd for $C_{57}{}^{13}C_3H_{59}N_2O_2OsP_4Rh$ ($M^{2+} - CF_3SO_3$), found 630.1148. Data for **17**: HRMS *m*/*z* found 630.1136 ($M^{2+} - CF_3SO_3$). Anal. Calcd for $C_{58}H_{56}F_6O_8OsP_5RhS_2$: C, 46.22; H, 3.75; S, 4.25. Found: C, 46.45; H, 3.88; S, 4.01. Compounds **16** and **17** decomposed when left in chlorinated solvents for extended periods of time.

*(i). Low-Temperature Protonation of Compounds **9** and **11** by HOTf.* At −78 °C, 1 equiv of HOTf was added to dark solutions containing either **9** (50 mg, 0.036 mmol) or **11** (50 mg, 0.037 mmol) in 0.7 mL of CD_2Cl_2, causing both solutions to immediately turn orange. Kept at this temperature, the NMR spectra indicated that only two species were present in solution; the major products were $[RhOs(L)(CO)_2(\mu\text{-}CH_3)(dppm)_2][CF_3SO_3]_2$ (L = IMe_4 (**12a**), PMe_3 (**13a**)), containing the *bridged agostic methyl groups*, while the minor products were the isomers **12b** (L = IMe_4) and **13b** (L = PMe_3), containing *terminal, Os-bound methyl groups*. These isomers were observed in an approximate 3:1 ratio in the case of PMe_3 and a 10:1 ratio in the case of IMe_4.

When the temperature was raised to 0 °C, the low-temperature products containing the IMe_4 ligand (**12a,b**) transformed into $[RhOs(CH_3)(CF_3SO_3)(L)(CO)(\mu\text{-}CO)(dppm)_2][CF_3SO_3]$ (L = IMe_4 (**14**)) via triflate ion coordination, while for the PMe_3-containing species the formation of the analogous triflate-coordinated species (**15**) occurred at −40 °C. Upon further warming to ambient temperature compound **14** transformed to $[RhOs(L)(CO)_2(\mu\text{-}CH_2)(\mu\text{-}H)(dppm)_2][CF_3SO_3]_2$ (L = IMe_4 (**16**)), while the PMe_3-containing species (**15**) transformed to an analogous methylene/hydride species (**17**) at 0 °C.

*(j). [RhOs(PMe$_3$)(CO)$_2$(μ-CH$_2$)(dppm)$_2$][BPh$_4$] (**11-BPh$_4$**).* To a slurry containing compound **2** (200 mg, 0.15 mmol) in 5 mL of THF was added 103 mg of $NaBPh_4$ (0.30 mmol). The solution was stirred for 30 min, and then the THF was removed in vacuo and the residue allowed to dry overnight under reduced pressure. A 5 mL portion of CH_2Cl_2 was added to the resulting residue, generating an orange solution and a white precipitate, which were separated by filtration through Celite. Compound **4** (as the BPh_4^- salt) was precipitated from the orange solution by the addition of 15 mL of pentane. ^{19}F NMR confirmed the absence of triflate ion. The ^{31}P, ^{13}C, and ^1H NMR spectra of this species were closely comparable to those of the compound having the triflate anion.[16] This compound was converted to **3-BPh$_4$** by addition of PMe_3, as reported for the triflate salt.[8c] To a 50 mg sample of **3-BPh$_4$** (0.032 mmol) in 0.7 mL of CD_2Cl_2 in an NMR tube was added 9.6 mg of TMNO (4 equiv). The solution was warmed to 39 °C in the NMR probe with constant monitoring. After 30 min the reaction was complete; leaving the mixture for longer periods resulted in decomposition. The resulting dark green solution was cooled in a dry ice/acetone bath followed by the addition of 1 mL of pentane to give a dark green oil. The yellow mother liquor was decanted to waste, and 1 mL of Et_2O was used to triturate the remaining oil. The light green ethereal solution was removed from the dark green solid, which was dissolved in 0.2 mL of CH_2Cl_2 and then precipitated using a 1.5 mL portion of Et_2O. The NMR parameters of **11-BPh$_4$** were in agreement with those of the triflate salt and are given in the Supporting Information.

*(k). Low-Temperature Protonation of **11-BPh$_4$** by [H(OEt$_2$)$_2$][BAr$^F_4$].* To a 50 mg portion (0.033 mmol) of **11-BPh$_4$** dissolved in 0.8 mL of CD_2Cl_2 was added 1 equiv of $[H(OEt_2)_2][BAr^F{}_4]$ at −80 °C. Monitoring the reaction by ^{31}P NMR spectroscopy showed no reaction at this temperature. Warming to −60 °C gererated the **13b** cation, and warming to −50 °C showed the appearance of the cation of **13a**, in an approximate 1:2.5 ratio. After 14 h at this temperature the new species **18** appeared, giving a 1:4:1 mix of **18**, **13a**, and **13b**. Warming to −30 °C resulted in the complete conversion of **13a,b** to **18**, which was stable upon warming to ambient temperature. The solvent was removed from the solution of **18** under reduced pressure, generating an orange oil. Dissolving this oil in 1 mL

of diethyl ether and adding 0.5 mL of pentane again yielded an orange oil, which was separated from the mother liquor via cannula and dried in vacuo. NMR characterization of this species showed large amounts of ether present, which resulted in unsatisfactory elemental analyses. HRMS: m/z calcd for $C_{56}H_{56}O_2P_5RhOs$ ($M^{2+} - BBh_4 - BAr^F{}_4 - OEt_2$) 605.0814, found 605.0813.

*(l). Reaction of [RhOs(Me)(OSO$_2$CF$_3$)(CO)$_3$(dppm)$_2$][CF$_3$SO$_3$] (**5**) with IMe$_4$.* To a rapidly stirred yellow solution consisting of 20 mg (0.01 mmol) of **5** in 0.7 mL of d_8-THF was added slightly less than 1 equiv of IMe_4 as a standardized THF solution, resulting in an instantaneous color change to dark red. Both ^{1}H and ^{31}P NMR spectra confirm the conversion to **2** with concomitant formation of [$HIMe_4$][OTf].

*(m). [RhOs(H)(IMe$_4$)(CO)(μ-CO)$_2$(dppm)$_2$][CF$_3$SO$_3$]$_2$ (**19a**).* At −78 °C, an excess of triflic acid (15 μL, 0.17 mmol) was added by syringe to a Schlenk flask containing compound **6** (200 mg, 0.14 mmol) in 5 mL of CH_2Cl_2. The orange solution immediately turned yellow, and 10 mL of −78 °C pentane was added via cannula to precipitate a yellow solid, which was removed from the mother liquor by decantation and dried in vacuo (203 mg, 92%). HRMS for **19a**: m/z calcd for $C_{61}H_{57}N_2O_6F_3P_4SRhOs$ ($M^{2+} - CF_3SO_3$) 1421.1510, found 1421.1513 ($M^{2+} - CF_3SO_3$).

*(n). [RhOs(IMe$_4$)(CO)$_2$(μ-H)(μ-CO)(dppm)$_2$][CF$_3$SO$_3$]$_2$ (**19b**)*

Method i. A 100 mg portion of **19a** (0.06 mmol) dissolved in 5 mL of CH_2Cl_2 was stirred for a 3 h period at ambient temperature, converting it fully to **19b**.

Method ii. An excess of triflic acid (15 μL, 0.17 mmol) was added by syringe to a Schlenk flask containing compound **6** (100 mg, 0.07 mmol) in 10 mL of CH_2Cl_2. The orange solution immediately turned pale yellow, and after 10 min of stirring 20 mL of Et_2O was added to precipitate a pale yellow solid, which was dried in vacuo (203 mg, 92%). Dissolving a portion of the crude product in CD_2Cl_2 revealed a 50:50 mixture of both bridging (**19b**) and terminal (**19a**) hydride isomers. Over a 3 h period at ambient temperature, **19a** converted fully to **19b**. Anal. Calcd for **19b**, $C_{62}H_{57}N_2O_9F_6P_4S_2RhOs$: C, 47.45; H, 3.66; N, 1.79. Found: C, 47.48; H, 3.73; N, 1.88.

X-ray Structure Determinations. *(a). General Considerations.* All data sets were collected using a Bruker SMART 1000 CCD detector/PLATFORM diffractometer[18] using Mo Kα radiation, with the crystals cooled to −80 °C. The data were corrected for absorption through use of a multiscan model (SADABS[18] (**6**) or TWINABS[18] (**8**)) or through Gaussian integration from indexing of the crystal faces[18] (**19b**). Structures were solved using direct methods (SHELXS-97[19] (**6**, **19b**)) or direct methods/structure expansion (SIR97[20] (**8**)). Refinements were completed using the program SHELXL-97.[19] Hydrogen atoms were assigned positions on the basis of the idealized sp^2 or sp^3 geometries of their attached carbon atoms and were given thermal parameters 20% greater than those of the attached carbons. See the Supporting Information for a listing of crystallographic experimental data.

(b). Data Collection and Structure Solution. (i) Yellow-orange crystals of compound **6** were grown via slow diffusion of CH_2Cl_2 into an Et_2O solution of the compound. Attempts to refine peaks of residual electron density as solvent Et_2O oxygen or carbon atoms were unsuccessful. The data were corrected for disordered electron density through use of the SQUEEZE procedure[21] as implemented in PLATON.[22] A total solvent-accessible void volume of 1174.0 Å^3 with a total electron count of 347 (consistent with eight molecules of solvent diethyl ether or two molecules per formula unit of the metal complex ion) was found in the unit cell.

(ii) Orange-red crystals of compound **8** were grown via diffusion of diethyl ether into a dichloromethane solution of the compound. The crystal used for data collection was found to display nonmerohedral twinning. Both components of the twin were indexed with the program CELL_NOW[18] (Bruker AXS Inc., Madison, WI, 2004). The second twin component can be related to the first component by 179.8° rotation about the [$-^1/_4$,1,0] axis in real space and about the [0,1,0] axis in reciprocal space. Integrated intensities for the reflections from the two components were written into a SHELXL-97 HKLF 5 reflection file with the data integration program SAINT (v. 7.06A),[18] using all reflection data (exactly overlapped, partially overlapped and nonoverlapped). The C−Cl and Cl···Cl distances of the disordered and/or partially occupied solvent dichloromethane molecules (distributed over three different sites) were restrained to be 1.80(1) and 2.77(2) Å, respectively.

(iii) Yellow crystals of compound **19b** were grown via diffusion of *n*-pentane into a CH_2Cl_2 solution of the compound. Attempts to refine peaks of residual electron density as solvent CH_2Cl_2 chlorine or carbon atoms were unsuccessful. The data were corrected for disordered electron density through use of the SQUEEZE procedure[21] as implemented in PLATON.[22] A total solvent-accessible void volume of 661.5 Å^3 with a total electron count of 102 was found in the unit cell, consistent with four molecules of solvent CH_2Cl_2 in the cell or two molecules of CH_2Cl_2 per formula unit of the complex dication. For further details of X-ray data collection and results for all structure determinations the reader is referred to the Supporting Information.

RESULTS AND COMPOUND CHARACTERIZATION

As noted in the Introduction, we set out to study the influence of the N-heterocyclic carbene, tetramethylimidazol-2-ylidene (L = IMe_4), on the equilibrium shown in eq 1 and in particular, to compare it to the case in which L = PMe_3. Our goal synthetically was to approach this problem from both sides of eq 1, first by protonation of the methylene-bridged precursors, namely [RhOs(L)(CO)$_3$(μ-CH$_2$)(dppm)$_2$]$^+$, and second by direct synthesis of the methyl products (**D**), either from methyl-containing precursors or by the introduction of methyl ligands into L-containing precursors.

$$\underset{\mathbf{C}}{[RhOs(H)L(CO)_3(\mu\text{-}CH_2)(dppm)_2]^{2+}} \rightleftharpoons \underset{\mathbf{D}}{[RhOsL(CO)_3(\mu\text{-}CH_3)(dppm)_2]^{2+}} \quad (1)$$

Two routes seemed obvious for accessing the methylene-bridged species [RhOs(L)(CO)$_3$(μ-CH$_2$)(dppm)$_2$]$^+$ (L = IMe_4, PMe_3; dppm = $Ph_2PCH_2PPh_2$), containing either the monophosphine or N-heterocyclic carbene as an ancillary ligand: (1) introduction of the bridging methylene group into the respective precursor complexes [RhOs(L)(CO)$_3$(dppm)$_2$]$^+$ (L = IMe_4, PMe_3) by reaction with diazomethane and (2) introduction of the ancillary ligands, IMe_4 or PMe_3, into either of the known methylene-bridged complexes, [RhOs(CO)$_3$(μ-CH$_2$)(dppm)$_2$]$^+$ or [RhOs(CO)$_4$(μ-CH$_2$)(dppm)$_2$]$^+$.[16]

IMe$_4$ and PMe$_3$ Precursors. Starting with the first route, the IMe_4 precursor [RhOs(IMe_4)(CO)$_3$(dppm)$_2$][OTf] (**6**) is readily accessed in near-quantitative yield by the careful addition of 1 equiv of IMe_4 to [RhOs(CO)$_4$(dppm)$_2$][OTf] (**1**), resulting in substitution of a Rh-bound carbonyl by the NHC ligand, as outlined in Scheme 1 (in this and all subsequent schemes, the phenyl rings on the dppm and derived groups are omitted in the drawings).

The ^{31}P{^{1}H} NMR spectrum of **6** displays a pattern characteristic of an AA′BB′X spin system, with one resonance at δ 29.4 appearing as a doublet of multiplets, having 132 Hz coupling to Rh, and the other as a multiplet at δ −3.5. The magnitude of the Rh coupling unambiguously establishes the low-field signal as that due to the pair of ^{31}P nuclei bound to this metal, leaving the upfield resonance, which displays no Rh coupling, as due to those bound to Os. In the ^{1}H NMR spectrum the resonance for the dppm methylene groups, at δ 3.58, appears

dx.doi.org/10.1021/om1010066 |*Organometallics* 2011, 30, 2654–2669

Scheme 1

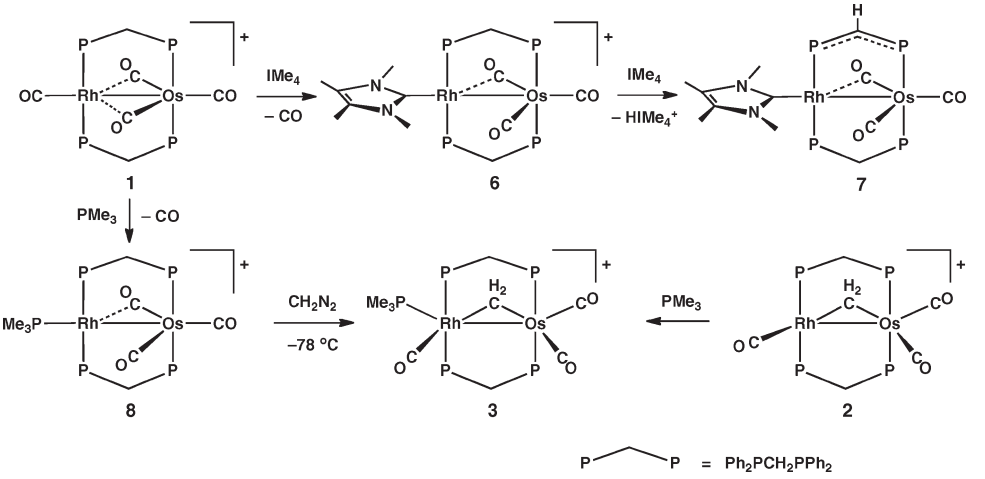

as an apparent quintet displaying essentially equal coupling to all ^{31}P nuclei. The appearance of a single dppm methylene resonance suggests the presence of front/back symmetry on either side of the $RhOsP_4$ plane, consistent with the IMe_4 ligand binding opposite the metal−metal bond, as shown. Selective decoupling at each individual phosphorus resonance in turn simplifies the methylene resonance to a triplet having coupling to the remaining phosphorus nuclei of 4.3 Hz in each case, while broad-band ^{31}P decoupling simplifies the resonance to a singlet. Further evidence for the front/back symmetry in the complex comes from the appearance of only two sharp singlets (integrating as six protons each) at δ 2.71 and 1.61, for the N-bound and C-bound methyl groups, respectively, of the imidazol-2-ylidene ring.

In the $^{13}C\{^1H\}$ NMR spectrum, the carbene carbon, at δ 176.4, appears as a doublet of triplets, showing typical coupling to rhodium[23,24] of 50 Hz and cis coupling of 16 Hz to the pair of adjacent Rh-bound phosphorus nuclei. The carbonyl resonances appear in a 2:1 intensity ratio at δ 216.2 and 183.7, respectively, with the former displaying 10 Hz coupling to Rh, suggesting a weak semibridging interaction with this metal for this pair of carbonyls, while the absence of Rh coupling for the high-field signal indicates an Os-bound carbonyl. However, a slightly different interpretation emerges upon consideration of the IR spectra, in which three carbonyl bands are observed in both solution and the solid state. Two stretches, at approximately 1967 and 1914 cm^{-1}, are assigned to two terminally bound carbonyls, while the lowest frequency band at 1785 cm^{-1} is attributed to a bridging carbonyl. The appearance of two terminal carbonyl stretches and only one bridging band in the IR spectra contradicts the above interpretation of the ^{13}C NMR experiments, which suggest that two carbonyls are bridging, leading us to propose a fluxional process that rapidly exchanges two of the carbonyls on the NMR time scale, while the faster time scale of the IR experiment allows the differentiation of these groups. We therefore suggest the static structure shown in Scheme 1, for which rapid exchange on the NMR time scale occurs. In this fluxional process the semibridging carbonyl, on one side of the $RhOsP_4$ plane, moves out of the bridge to a terminal position on Os while the terminal Os-bound carbonyl that lies on the opposite face of the $RhOsP_4$ plane moves to a semibridging position. Since a terminal Os-bound carbonyl is not expected to show resolvable coupling to ^{103}Rh, the average value (10 Hz) observed in the $^{13}C\{^1H\}$ NMR spectrum suggests a 20 Hz coupling for this carbonyl while bridging. This coupling to Rh is less than the 30 Hz expected for a symmetrically bridged CO,[16] and so it is attributed to a semibridging group.

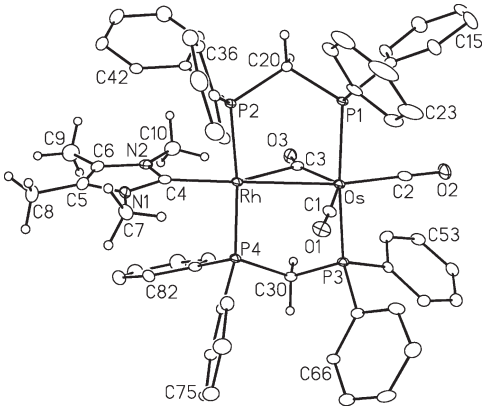

Figure 1. Perspective view of the complex cation of $[RhOs(IMe_4)(CO)_3(dppm)_2][CF_3SO_3]$ (**6**), showing the atom-labeling scheme. Phenyl carbon atoms are numbered sequentially around the ring, starting from the ipso carbon such that the first digit represents the ring number. Non-hydrogen atoms are represented by Gaussian ellipsoids at the 20% probability level, while hydrogen atoms are shown with arbitrarily small thermal parameters. Phenyl hydrogens are omitted for clarity. Relevant parameters (distances in Å and angles in deg): Os−Rh = 2.8303(4), Os−C(1) = 1.929(5), Os−C(2) = 1.889(5), Os−C(3) = 1.982(5), Rh−C(1) = 3.335(5), Rh−C(3) = 2.130(5), Rh−C(4) = 2.049(5); C(1)−Os−C(2) = 114.2(2), C(1)−Os−C(3) = 135.5(2), C(2)−Os−C(3) = 110.3(2), Os−C(3)−O(3) = 154.7(4), Rh−C(3)−O(3) = 118.0(4).

The X-ray crystal structure determination of **6** has been carried out, and the representation of the complex cation, shown in Figure 1, confirms the IR spectral assignment, displaying one semibridging and two terminal carbonyls. It should be noted that the reversible conversion of the terminally bound C(1)O(1) to a semibridging group accompanied by conversion of C(3)O(3) to terminal, as proposed above for the fluxional process, requires only slight movement of each carbonyl through a twisting of the "Os(CO)$_3$" fragment about the approximate P(1)−Os−P(3) axis. This structure also confirms that the NHC ring is bound to

dx.doi.org/10.1021/om1010066 |*Organometallics* 2011, 30, 2654–2669

Rh opposite the Rh−Os bond and shows that it lies in the equatorial plane defined by the metals and carbonyls, allowing the four NHC methyl substituents to avoid unfavorable interactions with the dppm phenyl rings.

The metal−metal separation of 2.8303(4) Å is consistent with the presence of a single bond, showing significant contraction compared to the intraligand P−P separations of 3.029(2) and 3.040(2) Å, while the Rh−C(4) distance of 2.049(5) Å is normal for a single bond, as shown for other NHC complexes,[23a,24] and is significantly longer than the metal−carbonyl distances. Carbonyl C(3)O(3) is identified as semibridging on the basis of the large asymmetry in the Rh−C(3)−O(3) and Os−C(3)−O(3) angles (118.0(4) and 154.7(4)°, respectively) and in the Rh−C(3) and Os−C(3) distances (2.130(5) and 1.982(5) Å, respectively), showing that this group is primarily bonded to Os while being involved in a weaker semibridging interaction with Rh. The observation of only two methyl resonances in the ^{1}H NMR spectrum of **6** is readily rationalized by the carbonyl fluxionality noted above but could also result from rotation about the Rh−IMe_4 bond. However, facile rotation about the Rh−carbene bond seems unlikely, owing to the severe repulsions that would appear to occur with the dppm phenyl groups.

The addition of another 1 equiv of IMe_4, in attempts to obtain a di-NHC complex (possibly having the second IMe_4 group on Os), instead gives a very different product (see Scheme 1), formulated as $[RhOs(IMe_4)(CO)_3(dppm\text{-}H)(dppm)]$ (**7**; dppm-H = bis(diphenylphosphino)methanide), resulting from deprotonation of one of the dppm methylene groups yielding $[HIMe_4][OTf]$ as the other product, which is observed in the ^{1}H NMR spectrum. The methylene groups of coordinated dppm are known to be acidic, and dppm-H species similar to **7** have previously been observed by us[25a−d] and others.[25e−k] Furthermore, the strong basicity of NHC ligands is also well recognized.[26] The $^{31}P\{^1H\}$ NMR spectrum of **7** shows four equal-intensity resonances at δ 34.2, 29.9, −4.6, and −6.2, for the four chemically unique phosphorus nuclei. Again the low-field resonances correspond to those bound to Rh, displaying 123 and 130 Hz coupling, respectively, to this metal. Simulation of this spectrum using SpinWorks[27] generates values of 345 and 188 Hz for the trans $^{31}P-^{31}P$ couplings observed across the Rh and Os centers, respectively, consistent with the values previously reported for a similar species, $[RhOs(CO)_4(dppm\text{-}H)(dppm)]$ ($^2J_{PP}$ = 321, 117 Hz).[25b] The derived 145 Hz intraligand-coupling ($^2J_{PP}$) within the dppm-H bridge is greater than the 87 Hz observed within the unaltered dppm group, consistent with π-delocalization over the deprotonated fragment of the former and in close agreement with previous observations.[25b−d] The ^{1}H NMR spectrum of **7** indicates that the symmetry about the $RhOsP_4$ plane is maintained, with only one resonance observed, at δ 3.26, for dppm methylene protons. In addition, the methanide dppm-H resonance, appearing at δ 2.51, is consistent with previous observations.[25a−c] The carbonyl region of the $^{13}C\{^1H\}$ NMR spectrum for **7** is similar to that observed for the parent complex **6**, displaying two resonances in a 2:1 intensity ratio at δ 218.2 ($^1J_{CRh}$ = 7 Hz, $^2J_{CP(Os)}$ = 9 Hz) and δ 188.1 ($^2J_{CP(Os)}$ = 13 Hz), respectively. As was shown for **6**, the IR spectrum of **7** also displays two terminal and one bridging carbonyl stretch (1960, 1906, and 1744 cm^{-1}), again suggesting a rapid exchange process of the two carbonyls on either side of the $RhOsP_4$ plane, as noted for **6**. The slightly lower frequencies of these stretches compared to those of the cationic precursor is consistent with increased electron density at the metal nuclei in the case of this neutral product. In all related compounds, the intermediate carbonyl stretch is somewhat low for a purely terminally bound group and probably results from a weak interaction with the adjacent metal.

As a comparison with the above IMe_4 compound (**6**), we have also prepared its PMe_3 analogue. Unlike the IMe_4 case, the addition of excess PMe_3 to **1** results in the exclusive formation of $[RhOs(PMe_3)(CO)_3(dppm)_2][OTf]$ (**8**) with no evidence of deprotonation products. The $^{31}P\{^1H\}$ NMR spectrum of **8** displays three resonances in a 2:2:1 ratio for the two ends of the pair of diphosphines and the PMe_3 ligand, respectively. The dppm resonances are very similar to those of the IMe_4 analogue (see Table 1), while the PMe_3 signal at δ −23.3 also appears, displaying typical coupling to Rh (144 Hz) and to the adjacent pair of Rh-bound ^{31}P nuclei of 40 Hz.

As was observed with compounds **6** and **7**, the $^{13}C\{^1H\}$ NMR spectrum of **8** shows two carbonyl resonances in a 2:1 ratio, while its IR spectrum displays carbonyl stretches at 1987, 1933, and 1771 cm^{-1}. On the basis of the spectral similarities of these compounds (particularly between **6** and **8**), a fluxional process that exchanges the semibridging and terminal Os-bound carbonyls on the NMR time scale is again proposed. Notably, the IR stretches for the terminal carbonyls in **8** are at higher frequency than for **6**, while that of the semibridging carbonyl is at slightly lower frequency. The first observation is consistent with IMe_4 being a better donor than PMe_3, while the reason for the lower frequency for the bridging carbonyl in **8** is not immediately obvious, although it should be noted that in our experience the carbonyl stretching frequency is not very diagnostic for identifying different types of bridging carbonyl modes (e.g., symmetrical, unsymmetrical, semibridging).

An X-ray structure determination of compound **8** was carried out, and the complex cation is represented in Figure 2, confirming the overall structural similarities with **6** while also pointing out the subtle differences. At a glance, the similarities in structure are obvious with the IMe_4 and PMe_3 groups bound to Rh, essentially opposite the Rh−Os bond. In addition, the structures of both confirm the single-carbonyl-bridged structure that was proposed on the basis of IR data.

The Rh−Os bonds in both compounds are also very similar (2.8303(4) Å (**6**), 2.8316(5) Å (**8**)). However, the very different shapes of the IMe_4 and PMe_3 ligands, with the former exerting a greater steric influence in the equatorial plane, perpendicular to the metal−phosphine vectors, and the probable electronic differences[12c] in the two, have noticeable effects on the bonding and positioning of the carbonyl ligands.

As noted earlier, on the basis of IR data, the IMe_4 ligand appears to be a better donor than PMe_3. This is manifested in a much stronger interaction of Rh with the semibridging carbonyl in compound **6** than in **8** (Rh−C(3) = 2.130(5), 2.281(5) Å, respectively), as a consequence of the more electron-rich Rh center in the former. The stronger attraction of C(3)O(3) to Rh in the IMe_4 complex (**6**) results in a twist of the trigonal arrangements of carbonyls about the P−Os−P vector in that direction, resulting in an increase in the nonbonding Rh−C(1) distance (3.114(6) Å in **8**, 3.335(5) Å in **6**) and an alignment of the axial carbonyl (C(2)O(2)) off the Rh−Os axis (Rh−Os−C(2) = 159.0(2)°) in compound **6**. This greater attraction of the semibridging CO for Rh in **6** occurs in spite of the greater steric demands of the adjacent IMe_4 group. It seems reasonable to expect that the greater size of IMe_4 in the plane of the carbonyls would result in it bending away from the semibridging CO. However, the IMe_4 group in **6** is aligned almost along the Os−Rh bond (Os−Rh−C(4) = 178.4(2)°), while the PMe_3 group in **8** is bent away from the bridging CO (Os−Rh−P(5) = 166.18(4)°). A

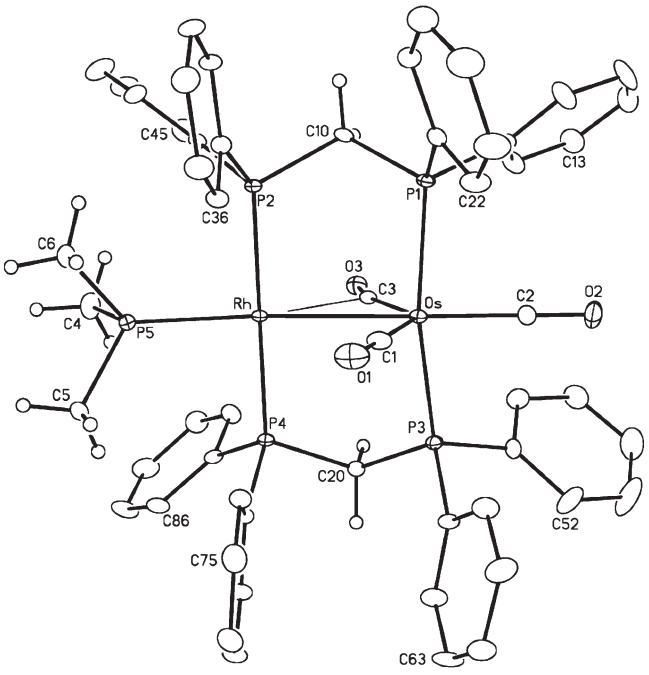

Figure 2. Perspective view of the complex cation of $[RhOs(PMe_3)(CO)_3(dppm)_2][CF_3SO_3]$ (**8**), showing the atom-labeling scheme. Atom numbering and thermal parameters are as described for Figure 1. Relevant parameters (distances in Å and angles in deg): Os−Rh = 2.8316(5), Os−C(1) = 1.919(6), Os−C(2) = 1.876(6), Os−C(3) = 1.950(5), Rh−P(5) = 2.3260(15), Rh−C(1) = 3.114(6), Rh−C(3) = 2.281(5); C(1)−Os−C(2) = 107.3(3), C(1)−Os−C(3) = 132.6(2), C(2)−Os−C(3) = 120.1(3), Os−C(3)−O(3) = 163.8(5), Rh−C(3)−O(3) = 112.5(4).

consideration of the structures reveals that these orientations are related more to the dppm phenyl group orientations than to the equatorial ligand positions. In **8** the more conical shape of PMe_3 interacts strongly with phenyl rings 4 and 8, forcing the phosphine off the Rh−Os axis, while for **6** the more planar IMe_4 group allows the corresponding phenyl rings to lie more horizontally, creating less repulsion.

Methylene-Bridged Complexes. As noted earlier, the next step in generating methylene-bridged species was to react the IMe_4 and PMe_3 precursors (**6** and **8**) with diazomethane. Although the related tetracarbonyl complex **1** has a rich chemistry with diazomethane,[16] displaying reactivity even at −80 °C, the NHC analogue **6** is unreactive toward diazomethane, even at elevated temperatures, failing to yield the methylene-bridged, IMe_4-containing target by this route. The PMe_3 analogue **8**, on the other hand, reacts readily with diazomethane, although a mixture of unidentified products is obtained at ambient temperature, as determined by ^{31}P NMR spectroscopy. However, the methylene-bridged target, $[RhOs(PMe_3)(CO)_3(\mu\text{-}CH_2)(dppm)_2][OTf]$ (**3**), can be obtained quantitatively by carrying out the reaction at −78 °C (see Scheme 1); this product was previously prepared by PMe_3 addition to the methylene-bridged precursors $[RhOs(CO)_x(\mu\text{-}CH_2)(dppm)_2]^+$ (x = 3, 4).[8c] The products observed in the ambient-temperature reaction of **8** with diazomethane were not investigated further. We suggest that the failure of **6** to react with diazomethane is due to the steric dominance of the IMe_4 group in the equatorial plane, preventing prior coordination of CH_2N_2.

Scheme 2

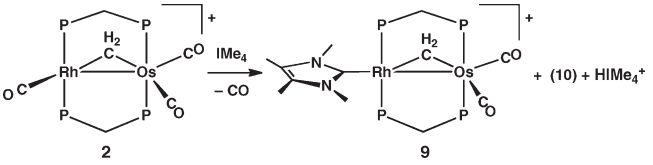

The second possible route for generating an IMe_4-containing, methylene-bridged target, namely the introduction of the NHC to a pre-existing methylene-bridged species, as noted above for PMe_3 and reported for other phosphines,[8c] was also attempted for IMe_4. Addition of IMe_4 to the tricarbonyl, methylene-bridged species **2**, as shown in Scheme 2, does yield a methylene-bridged, IMe_4-containing species, $[RhOs(IMe_4)(CO)_2(\mu\text{-}CH_2)(dppm)_2][OTf]$ (**9**), but unlike the case for the PMe_3 analogue, the simple adduct is not formed. Instead, substitution of one carbonyl has occurred, presumably due to the significantly increased steric bulk of IMe_4 in the equatorial plane that labilizes the Rh-bound carbonyl. Furthermore, in this case the methylene-bridged product (**9**) is obtained as the minor product together with the unexpected coproduct $[RhOs(CO)_3(\mu\text{-}CH_2)(\mu\text{-}\kappa^1\text{:}\eta^2\text{-}Ph_2PCHPPh_2)(dppm)]$ (**10**) in a 1:4 ratio—the latter species resulting from competing Brønsted−Lowry acid/base chemistry through deprotonation of a dppm methylene group by IMe_4. Repeating the reaction at −78 °C reverses the relative abundance of these species, giving an approximate 3:1 ratio of **9** and **10**, and separation of these species is described in the Experimental Section. The deprotonation product **10** can be generated quantitatively by the reaction of **2** with the strong base $KN(Si(CH_3)_3)_2$ but is not discussed further here, since its chemistry is the topic of another paper.[25d]

A satisfactory elemental analysis for complex **9** could not be obtained, as attempts to fully remove residual imidizolium salt were unsuccessful; however, high-resolution mass spectrometry and multinuclear NMR spectroscopy (see the Supporting Information) agree with the assigned formulation. The $^{31}P\{^1H\}$ NMR spectrum displays two resonances, in which the Rh-bound ends of the diphosphines appear at δ 25.0 displaying 132 Hz coupling to rhodium, while the Os-bound ends appear at δ −2.66. The front/back asymmetry across the approximate $RhOsP_4$ plane, a consequence of the bridging CH_2 group, gives rise to four chemically unique methyl resonances for the IMe_4 ligand (δ 3.14, 2.90, 2.63, and 1.47) in the ^1H NMR spectrum, while the dppm methylene groups appear as two signals at δ 4.55 and 3.97. The methylene group bridging the metals appears downfield in the ^1H NMR spectrum at δ 8.71 as a triplet of triplets and displays unsymmetrical coupling to the Rh- (5.5 Hz) and Os-bound (15.4 Hz) ^{31}P nuclei, as confirmed by selective ^{31}P decoupling experiments. This coupling pattern suggests that the μ-CH_2 group is more strongly bound to osmium, possibly a result of steric repulsion involving the bulky Rh-bound IMe_4 group. In the ^{13}C NMR spectrum, this bridging methylene group appears at δ 121.3, displaying typical coupling to rhodium of 19 Hz[8c,16] and a one-bond C−H coupling of 138 Hz. Interestingly, both the ^1H and ^{13}C chemical shifts for the bridging methylene group in compound **9** are significantly downfield from those observed in the closely related, but more coordinatively saturated, methylene-bridged compounds, in which the NHC group is replaced by a pair of carbonyls or a monophosphine and a carbonyl.[8c] The two carbonyls, observed at δ 188.5 and 184.3 in the $^{13}C\{^1H\}$ NMR spectrum, are terminally bound to osmium,

Scheme 3

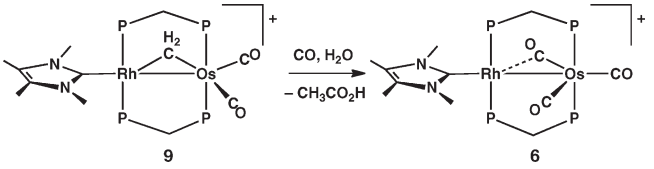

9 6

Scheme 4

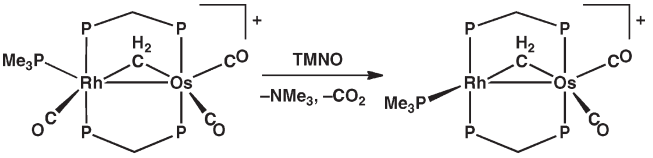

3 11

as shown by the absence of Rh coupling and the observed coupling to the adjacent Os-bound ends of the diphosphines. The $^{13}C-^{13}C$ coupling constant of 11 Hz, observed between the downfield carbonyl and the bridging methylene group, in the $^{13}CO/^{13}CH_2$-enriched sample, suggests that these groups are mutually trans. The carbene carbon of the NHC group, observed at δ 179.7, displays coupling to rhodium of 48 Hz, while the IMe_4 methyl groups appear as singlets at δ 34.6, 33.7, 8.2, and 8.1, further demonstrating their chemical inequivalence.

Methyl Complexes. *(a). Protonation of Methylene-Bridged Species.* Having in hand methylene-bridged complexes of IMe_4 (**9**) and PMe_3 (**3**), we set out to compare their protonations. However, the IMe_4-containing, methylene-bridged product **9** has one less carbonyl ligand than the known PMe_3 complex **3**, complicating any direct comparison of their chemistries. Attempts to generate the carbonyl adduct of **9**, which would be directly comparable to **3**, did not succeed, resulting instead in loss of the methylene group to give **6** (see Scheme 3). In this transformation the methylene group is presumably lost as ketene, although this product is not observed. Its involvement is proposed on the basis of the observation of acetic acid in solution, which presumably results by the reaction of ketene with adventitious water. When the reaction was carried out using ^{13}CO, partial ^{13}C incorporation was observed in the acetic acid formed.

Having been unable to generate the IMe_4 analogue of **3**, we instead generated the PMe_3 analogue of **9**, namely $[RhOs(PMe_3)(CO)_2(\mu\text{-}CH_2)(dppm)_2][CF_3SO_3]$ (**11**), by reaction of **3** with trimethylamine *N*-oxide (TMNO), as outlined in Scheme 4. The $^{31}P\{^1H\}$ NMR spectrum of **11** displays three signals in a 2:2:1 ratio, in which the Rh-bound ends of the diphosphines appear at δ 25.7, displaying 130 Hz coupling to rhodium and 38 Hz coupling to the PMe_3 group, the Os-bound ends appear at δ 2.02, and the PMe_3 signal appears at δ −24.4, displaying typical coupling to Rh (122 Hz) and to the adjacent pair of Rh-bound ^{31}P nuclei, noted above. The methylene group bridging the metals, which appears downfield in the ^1H NMR spectrum at δ 7.09 as a triplet of triplets of doublets, displays unsymmetrical coupling to the Rh-bound (7.2 Hz) and Os-bound (14.5 Hz) ^{31}P nuclei, as confirmed by ^{31}P decoupling experiments, and coupling to ^{103}Rh of 2.6 Hz. As was the case for **9**, this coupling pattern suggests that the μ-CH_2 group is more strongly bound to osmium. In the ^{13}C NMR spectrum, this bridging methylene group is also downfield, at δ 105.7, displaying coupling to rhodium of 17 Hz[8c,16] and one-bond C−H coupling of 133 Hz. The two carbonyls, observed at δ 187.3 and 180.2 in the $^{13}C\{^1H\}$ NMR spectrum, are terminally bound to osmium, as shown by the absence of Rh coupling and their coupling to the Os-bound ends of the diphosphines. For the low-field carbonyl an additional 12 Hz coupling is observed to the μ-$^{13}CH_2$ group, suggesting a mutually trans arrangement of these groups.

As outlined in Scheme 5, protonation of the IMe_4 complex **9** by HOTf at −78 °C yields a pair of isomers, $[RhOs(CH_3)(IMe_4)(CO)_2(dppm)_2][CF_3SO_3]_2$ (**12a**,**b**), in an approximate 10:1 ratio, while protonation of the PMe_3 analogue **11** yields the corresponding pair of isomers **13a**,**3b** in a 2:1 ratio. The protonations of compounds **9** and **11** proceed in parallel, as shown in Scheme 5, and the spectral parameters for the IMe_4 and PMe_3 series of compounds are quite comparable (in all cases the resonances for the dppm, IMe_4, and PMe_3 groups are as expected and so are not discussed here). The reactivities of compounds **9** and **11** differ only in the relative concentrations of the pairs of isomers produced at −78 °C (**12a**,**b** or **13a**,**b**) and in the temperatures at which conversions to subsequent products occur.

In both systems the differences in the **a** and **b** isomers relate mainly to the bonding of the methyl and carbonyl groups. Unfortunately, the methyl resonances, in both the ^{13}C and ^1H NMR spectra, are broad over the accessible temperature range, obscuring much of the spin−spin coupling information. Nevertheless, the significant differences in these isomers are obvious from the available data. For the **a** isomers, the $^{13}C\{^1H\}$ NMR resonances for the methyl groups appear at δ 7.9 (**12a**) and −6.0 (**13a**) with the ^1H resonances appearing at δ 0.08 (**12a**) and −0.74 (**13a**). In the proton-coupled ^{13}C NMR spectra of $^{13}CH_3$-enriched samples, one-bond C−H coupling of 111 Hz (**12a**) and 117 Hz (**13a**) is observed. This coupling is much lower than is typical for a terminal methyl group[28] (for example, see compounds **14** and **15**, for which $^1J_{CH}$ = 133 Hz) and instead results from an unsymmetrically bridged methyl group in which the three hydrogens are exchanging rapidly. The values observed correspond to the weighted average of two terminal C−H bonds and the bridging (agostic) C−H interaction. In unsymetrically bridged methyl groups the coupling constants ($^1J_{CH}$) involving the nonbridged bonds are often observed near 140 Hz.[8c] Using this value for terminal C−H coupling, the agostic interaction can be approximated at 53 Hz in the case of IMe_4 and 71 Hz in the case of PMe_3—values that represent a substantial weakening of this C−H bond owing to a strong interaction with the adjacent metal. These values also suggest that the IMe_4 ligand provides a more electron-rich Rh center in comparison to PMe_3 with concomitant increased back-donation to the C−H σ^* orbital.

Protonation of the PMe_3 compound **11**, using a sample of DOTf that was contaminated by HOTf, gave rise to two resonances in the ^1H NMR spectrum at δ −0.74 and −0.95 for the CH_3 and CH_2D groups, respectively, of **13a**; the observed isotope shift is consistent with the presence of the IPR phenomenon, as has been well documented,[1c,4a,4e,8a,8c,28] supporting the bridged, agostic structure.

In the $^{13}C\{^1H\}$ NMR spectra of **12a** and **13a**, both species display two terminal Os-bound carbonyls, at δ 183.4 and 169.6 for **12a** and at δ 182.0 and 169.0 for **13a**, each displaying coupling to the pair of adjacent ^{31}P nuclei; in addition, two-bond coupling (11 Hz (**12a**) and 12 Hz (**13a**)) between the low-field carbonyl and the Os-bound methyl group is also observed, suggesting a mutually trans arrangement. Similar $^2J_{CC}$ values, involving the μ-CH_2 and

dx.doi.org/10.1021/om1010066 |*Organometallics* 2011, 30, 2654–2669

Scheme 5

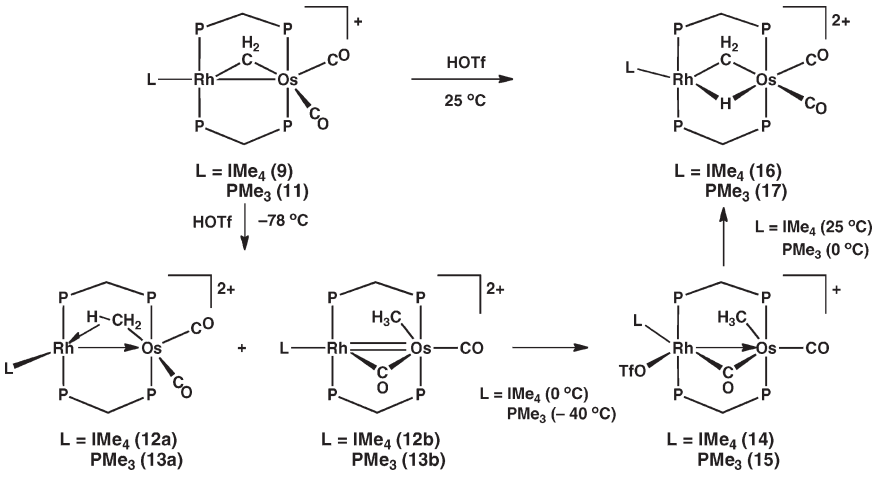

low-field carbonyl, were observed in the parent species **9** and **11**, suggesting little change in geometry upon protonation. A dative Rh→Os(II) bond is proposed for isomers **12a** and **13a** in order for Os to achieve its favored 18e configuration. The structures of these isomers very much resemble that of the kinetic product in the protonation of $[RhOs(CO)_3(\mu\text{-}CH_2)(dppm)_2]^+$, with the exception that triflate ion coordination was observed for this tricarbonyl product.[8c] In contrast, the ^{19}F NMR spectra of the **12a,b** and **13a,b** mixtures indicate that triflate ion coordination has not occurred in any of these species, with only free triflate ion at δ −78.8 in the ^{19}F NMR spectrum being observed.

As noted, the major differences between isomers **a** and **b** are seen in the parameters for the methyl and carbonyl groups. For isomers **12b** and **13b** one carbonyl on each is terminal (δ 178.8 (**12b**) and 179.5 (**13b**)), displaying coupling to only the Os-bound ^{31}P nuclei. However, for these isomers the other carbonyl is bridging, as seen by its downfield shift (δ 203.6 (**12b**) and 193.6 (**13b**)) and its coupling to ^{103}Rh (23 and 18 Hz, respectively). In the proton-coupled ^{13}C NMR spectra, the $^{13}CH_3$ groups are observed at δ −28.8 (**12b**) and −29.2 (**13b**), displaying significantly larger one-bond C−H coupling of 125 Hz (**12b**) and 126 Hz (**13b**) than for the **a** isomers. This coupling is within the "normal" range for terminally bound methyl groups (125−140 Hz)[28] and in addition, in the experiment described earlier in which the protonation of **11** was carried out using a HOTf/DOTf mixture, the small isotope shift for **13b-CH$_3$** (δ 0.93) compared to that for **13b-CH$_2$D** (δ 0.90) is typical for geminal substitution of H by D[29] and is too small for the IPR effect, arguing against any significant bridging arrangement for this group. Although the protonation of **9** using DOTf was not carried out, the ^1H NMR resonance for the methyl group in **12b** (δ 1.60) is typical for a terminal group. For isomer **13b**, an additional 34 Hz coupling between the methyl carbon and the ^{31}P nucleus of PMe_3 is observed. Although three-bond $^{13}C-^{31}P$ coupling is typically not this large,[30] particularly when these groups occupy different metals, we have previously observed a number of cases in which such coupling through the metal−metal bond has been observed.[8c,31]

As shown in Scheme 5, warming solutions of **12a,b** to 0 °C or of **13a,b** to −40 °C results in the conversion of both sets of isomers to the terminally bound methyl species $[RhOs(CH_3)(OSO_2CF_3)(L)(CO)(\mu\text{-}CO)(dppm)_2][CF_3SO_3]$ (L = IMe_4(**14**), PMe_3 (**15**)). Now coordination of a $CF_3SO_3^-$ anion is clear, as seen by the appearance of coordinated triflate, at δ −77.3 (**14**) and δ −76.7 (**15**), together with free triflate ion in the ^{19}F NMR spectrum. In both compounds the methyl ligand appears in the ^1H NMR spectrum as a triplet, at δ 0.18 (**14**) and at δ 0.06 (**15**), displaying 6.3 and 6.8 Hz coupling, respectively, to the Os-bound ^{31}P nuclei. Notably, in $^{13}CH_3$-enriched samples an additional 133 Hz coupling to carbon is observed in both cases; this value is normal for a terminal methyl group.[28] In the ^{13}C NMR spectra, the bridging carbonyl groups, at δ 205.9 (**14**) and 199.5 (**15**), show strong 39 Hz (**14**) and 40 Hz (**15**) coupling to ^{103}Rh, together with an additional trans coupling of 40 Hz to the $^{31}PMe_3$ ligand in compound **15**. The terminally bound carbonyls, at δ 177.6 (**14**) and 176.3 (**15**), show the expected coupling to the Os-bound ends of the dppm groups and 4 Hz coupling to the $^{13}CH_3$ group consistent with a mutually cis arrangement. The $^{13}CH_3$ resonance appears as a quartet at δ 13.8 (**14**) and 14.5 (**15**) in the ^{13}C NMR spectra.

Further warming of compound **14** to ambient temperature or of compound **15** to 0 °C yields the final products, $[RhOs(L)(CO)_2(\mu\text{-}CH_2)(\mu\text{-}H)(dppm)_2][CF_3SO_3]_2$ (L = IMe_4 (**16**), PMe_3 (**17**)), containing bridging methylene and hydride groups; these are the only products observed on protonation of **9** or **11** at ambient temperature. In the ^1H NMR spectra the bridging methylene groups appear as pseudoquintets with coincidental 8.5 Hz (**16**) and 6.0 Hz (**17**) coupling to the inequivalent sets of Rh- and Os-bound ^{31}P nuclei, confirming their bridging arrangement, and in $^{13}CH_2$-labeled samples an additional 133.7 (**16**) and 138.7 Hz (**17**) one-bond coupling to the ^{13}C nucleus is observed. As is often the case, two-bond coupling to ^{103}Rh is not observed in these ^1H signals. The resonances assigned to the bridging hydride of **16** (δ −11.47) and of **17** (δ −10.90) appear as complex multiplets, due to coupling to the four (**16**) or five (**17**) ^{31}P nuclei, to ^{103}Rh, and (in a ^{13}CO-enriched sample) to both Os-bound carbonyls. Upon broad-band ^{31}P decoupling, these hydride resonances simplify to a doublet of doublets with 14.8 Hz (**16**) and 15.0 Hz (**17**) coupling to ^{103}Rh and 7 Hz coupling to the trans carbonyl appearing at δ 173.2 (**16**) and 176.4 (**17**) in the $^{13}C\{^1H\}$ NMR spectra. In the case of **17**, 60 Hz two-bond coupling of the hydride resonance to the PMe_3 group is also observed, suggesting a trans arrangement of these groups across Rh. For both compounds (**16** and **17**) two Os-bound carbonyl resonances are observed, one of which displays 14−15 Hz trans

dx.doi.org/10.1021/om1010066 |*Organometallics* 2011, 30, 2654–2669

coupling to the bridging methylene groups, which appear at δ 99.6 (**16**) and 79.4 (**17**) and display 32 and 36 Hz coupling to Rh, respectively.

We have also investigated the protonation of $[RhOs(PMe_3)(CO)_2(\mu\text{-}CH_2)(dppm)_2][BPh_4]$ (**11-BPh$_4$**), in which the triflate ion in **11** has been replaced by the noncoordinating BPh_4^- anion and in which the acid $[H(OEt_2)_2][BAr^F{}_4]$, also containing a noncoordinating anion, was used. In this case, no reaction is observed at −80 °C, but warming to −60 °C yields the complex cation of **13b**, having NMR spectral parameters very similar to those of the triflate salt (see the Supporting Information for spectra). Although protonation of **11** by triflic acid yielded both **13a** and **13b** at −80 °C, **13a** does not appear together with **13b** when $[H(OEt_2)_2][BAr^F{}_4]$ is used but appears on subsequent warming to −50 °C. After 14 h at this temperature species **13a,b** have apparently reached their equilibrium concentrations, while a new species (**18**) has also emerged, giving a **13a**:**13b**:**18** ratio of 4:1:1. Further warming to −30 °C results in the complete transformation of **13a,b** into **18**, which is stable upon warming to ambient temperature. Compound **18** is formulated as $[RhOs(CH_3)(PMe_3)(CO)_2(OEt_2)(dppm)_2]^{2+}$, having BPh_4^- and $BAr^F{}_4^-$ counterions.

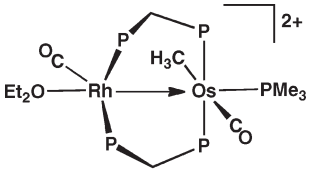

18

The transformation of the **13a,b** mix to **18** has been accompanied by the migration of PMe_3 to Os and of a carbonyl to Rh. In addition, the methyl ligand is terminally bound to Os, as seen by its lack of coupling to Rh in the ^{1}H and ^{13}C NMR spectra and its coupling to the Os-bound ^{31}P nuclei. In the $^{31}P\{^1H\}$ NMR spectra five resonances are observed for the chemically inequivalent ^{31}P nuclei; the pair on Rh are shown by their mutual coupling of 46 Hz to be mutually cis, while the Os-bound ends of the dppm groups display trans coupling of 219 Hz. The inequivalence of the ^{31}P nuclei on each metal is presumed to arise from a twisting about the Rh−Os bond, which places them in inequivalent environments. At ambient temperature only one set of broad resonances for ether is observed, however, upon cooling to −80 °C resonances for the coordinated ether appear at δ 3.98 and 1.33, together with free ether. On the basis of the spectroscopy summarized in Table 1, compound **18** is assigned the structure shown. Although the exact geometry is not known, the connectivity seems clear and the binding of the methyl group terminally to Os is unambiguous. No evidence was seen for a methylene/hydride species, as was observed in the triflic acid protonation.

(b). Other Possible Routes to Methyl Species. Two additional direct routes to the target IMe_4/methyl species were also attempted. In the first we attempted to replace the labile Os-bound triflate anion in the known species $[RhOs(Me)(OSO_2CF_3)(CO)_3(dppm)_2][CF_3SO_3]$ (**5**)[8c] by IMe_4. However, in parallel to the case observed earlier, the Brønsted−Lowry basicity of IMe_4 again dominates, leading instead to deprotonation of the methyl ligand to yield the known species **2** and $[HIMe_4][OTf]$, as outlined in Scheme 6.

Another potential route to an IMe_4/methyl complex of the type targeted is the reaction of $[RhOs(IMe_4)(CO)_3(dppm)_2]^+$ (**6**) with methyl triflate. However, no reaction between these

Scheme 6

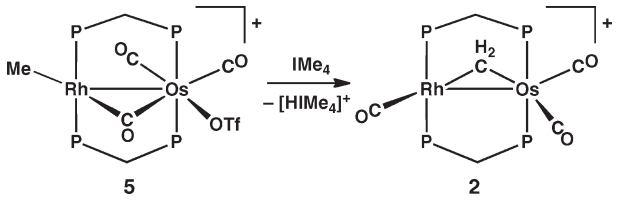

5 **2**

species was observed, even in an excess of methyl triflate. Attempts to generate the known PMe_3 analogue $[RhOs(Me)(PMe_3)(CO)_3(dppm)_2]^{2+}$ by reaction of $[RhOs(PMe_3)(CO)_3(dppm)_2]^+$ (**8**) with methyl triflate also failed, with no reaction observed. Presumably the methyl triflate is too weak an electrophile to react with these cationic species.

Hydride Products. Although compound **6** did not react with methyl triflate, it is readily protonated by triflic acid, yielding the kinetic product **19a** when carried out at −78 °C. This species slowly converts to the thermodynamic product **19b** over the course of several hours at ambient temperature. Compounds **19a,b** are formulated as isomers of the monoprotonation product, $[RhOs(H)(IMe_4)(CO)_3(dppm)_2][CF_3SO_3]_2$, as shown in Scheme 7. Their $^{31}P\{^1H\}$ NMR spectra are as expected for the proposed structures (see Table 1). In the ^{1}H NMR spectrum, the hydride resonance for **19a**, located at δ −5.94, shows coupling to only the adjacent Os-bound ^{31}P nuclei, indicating that it is terminally bound to this metal. The $^{13}C\{^1H\}$ NMR spectrum shows three unique carbonyl environments; two are found to be bridging, while one (a triplet at δ 173.8 ($^2J_{CP}$ = 9 Hz)) is terminally bound to Os. One of the bridging carbonyls, at δ 211.4, displays coupling of 24 Hz to Rh, while the other, at δ 198.6, appears as a doublet of triplets, having 18 Hz coupling to ^{103}Rh and 3.5 Hz coupling to the Os-bound ends of the diphosphines. On the basis of the coupling constants, both appear to be semibridging, although with the former interacting somewhat more strongly with Rh. The $^{13}C\{^1H\}$ NMR spectrum also shows the carbene carbon at δ 161.7 with coupling to both Rh (63 Hz) and the Rh-bound ^{31}P nuclei (19 Hz).

From ^{1}H NMR spectroscopy it is clear that the thermodynamic product **19b** is a hydride-bridged species, displaying the hydride resonance in the ^{1}H NMR spectrum at δ −10.91 as a doublet of triplet of triplets, having coupling to ^{103}Rh of 18.8 Hz, and to the Rh- and Os-bound ^{31}P nuclei of 9.3 and 7.3 Hz, respectively. In the $^{13}C\{^1H\}$ NMR spectrum, the two terminal carbonyls bound to osmium appear as triplets at δ 176.7 and 171.6, with coupling to the Os-bound phosphorus nuclei, while the third carbonyl appears as a complex multiplet, at δ 223.5, displaying coupling to all phosphorus nuclei and to Rh. Broad-band decoupling ($^{13}C\{^{31}P, ^1H\}$) simplifies this resonance to a doublet displaying 29 Hz coupling to rhodium, typical of a symmetrically bridged carbonyl. Compounds **19a,b** are readily deprotonated by addition of triethylamine, regenerating **6**.

The structure for the complex dication **19b** is shown in Figure 3 and unambiguously confirms the spectroscopic assignments. Protonation of **6** has resulted in lengthening of the metal−metal separation from 2.8303(4) Å to 2.9030(3) Å, consistent with the conversion of a two-center, two-electron Rh−Os bond to a three-center, two-electron Rh−H−Os bond. The resulting geometry at Os is best described as octahedral, while that at Rh appears as a tetragonal pyramid having the bridging carbonyl (C(3)O(3)) at the apical site. Protonation at the metal−metal

dx.doi.org/10.1021/om1010066 |*Organometallics* 2011, 30, 2654–2669

Scheme 7

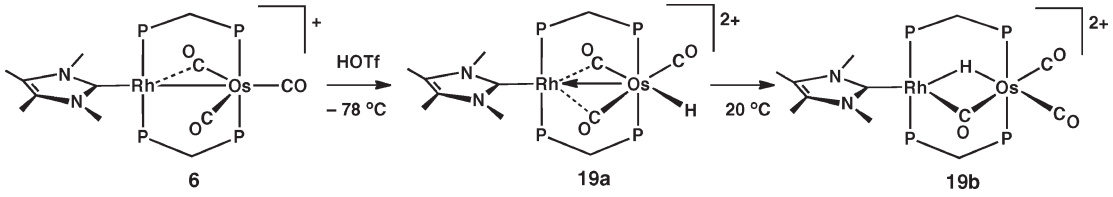

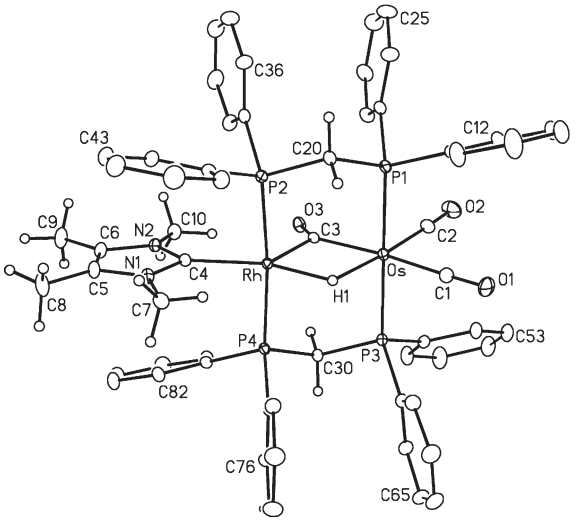

Figure 3. Perspective view of the complex dication of $[RhOs(IMe_4)(CO)_2(\mu\text{-}H)(\mu\text{-}CO)(dppm)_2][CF_3SO_3]_2$ (**19b**), showing the atom-labeling scheme. Atom numbering and thermal parameters are as described for Figure 1. Relevant parameters (distances in Å and angles in deg): Os–Rh = 2.9030(3), Os–C(3) = 2.082(3), Os–C(2) = 1.923(3), Os–C(1) = 1.934(3), Os–H(1) = 1.85(4), Rh–C(4) = 2.043(3), Rh–C(3) = 2.026(3), Rh–H(1) = 1.79(4); C(3)–Os–C(2) = 93.82(13), C(2)–Os–C(1) = 92.73(14), C(1)–Os–H(1) = 92.8(12), H(1)–Os–C(3) = 80.6(12), C(4)–Rh–C(3) = 118.67(11), C(3)–Rh–H(1) = 83.4(13), C(4)–Rh–H(1) = 157.8(13), Os–C(3)–O(3) = 143.1(2), Rh–C(3)–O(3) = 126.8(2).

bond has also forced the IMe_4 and CO ligands away from this protonation site such that the Os–Rh–C(4) angle observed for **6** (178.4(2)°) has decreased to 164.45(8)°, while the Rh–Os–C(1) angle has opened up from 86.8(1)° to 129.3(1)° upon protonation. Protonation has also resulted in a compression of the intercarbonyl angles to near 93°, reflecting the nearly octahedral geometry at Os. Other structural changes upon protonation of **6** reflect the changes in orientation of the dppm phenyl rings (particularly those on P(1) and P(2)) in order to minimize nonbonding contacts with the carbonyl and IMe_4 ligands in the equatorial plane. Interestingly, the close-to-trans arrangement of the bridging hydride and the IMe_4 group in **19b** is the geometry suggested earlier, on the basis of NMR evidence, for the PMe_3 and hydride groups in **17**.

An alternate potential route to methyl-containing products involving the reaction of the hydride-bridged species **19b** with diazomethane, in hope of bringing about insertion of the diazomethane-generated methylene group into one of the metal-hydride bonds, gave no reaction, even after extended periods. Presumably, the saturation at Os and steric crowding at Rh, preventing diazomethane attack, are two factors inhibiting reaction.

DISCUSSION

The similarities between the two ligand classes (PR_3 and NHC) notwithstanding, there remain significant differences between the two, some of which are demonstrated in this study. The steric differences between the two ligand types[12d] are widely recognized, and in this study the pseudoplanar IMe_4 ligand exerts a significantly greater steric influence in the equatorial plane of the binuclear complexes (perpendicular to the μ-dppm groups) than the more conical PMe_3 group. This greater "equatorial presence" is presumably the reason that the IMe_4 analogue of $[RhOsL(CO)_3(\mu\text{-}CH_2)(dppm)_2]^+$ (L = CO, PMe_3) could not be prepared, owing to the labilization of the third carbonyl ligand by the larger IMe_4 group. Furthermore, the failure of diazomethane to react with $[RhOs(IMe_4)(CO)_3(dppm)_2]^+$, even at above-ambient temperatures, is in marked contrast to the facile reactivity of the PMe_3 and CO analogues at −80 °C and is rationalized on the basis that the larger IMe_4 group prevents diazomethane access to the metals.

However, the most significant difference between IMe_4 and PMe_3 to emerge from this study is the significantly greater tendency of the former to function as a Brønsted base, as demonstrated by its facile deprotonation of either dppm or methyl ligands. NHC ligands are known to deprotonate acidic hydrocarbons,[26c,32] and so the deprotonation of the acidic dppm methylene group,[25] although not anticipated, was not surprising. On the other hand, deprotonation of a methyl ligand *was* surprising, and in particular its deprotonation in preference to the dppm groups was unexpected. Certainly, however, dppm deprotonation by IMe_4 has been a recurring theme throughout our recent studies on this and related dppm-bridged systems.[25c,d]

Given this tendency for IMe_4 to function as a Brønsted base, we investigated the protonation of $[RhOs(IMe_4)(CO)_3(dppm)_2]^+$ (**6**) in order to determine whether elimination of $HIMe_4^+$ from the metals would occur. Reductive elimination of NHC groups with either hydrido or alkyl ligands has been observed previously,[33] and in at least one case, reductive elimination of the imidizolium salt was induced by protonation of the NHC complex.[33b] The kinetic product of protonation, in our study $[RhOsH(IMe_4)(CO)_3(dppm)_2]^{2+}$ (**19a**), has the hydrido and NHC ligands on different metals, where they are not appropriately placed for a reductive elimination, while the thermodynamic isomer (**19b**) has the hydrido ligand bridging the metals. Although in this product both the hydrido and NHC groups are bound to Rh, their mutually trans arrangement is again not conducive to reductive elimination; consequently, no elimination is observed.

Our original goal in this study was to determine the influence of the IMe_4 ligand on the position of the tautomeric equilibrium between the unsymmetrically bridged methyl species **D** and the methylene/hydride **C**, shown in eq 1. In an earlier study the anticipation that a basic ligand (PR_3) would favor the methylene/hydride species, as had been observed by Shapley and co-workers

in Os_3 clusters,[11] had not materialized in our Rh/Os series. Nevertheless, we considered that the greater basicity of IMe_4 might favor the methylene/hydride species. One approach to such products was through protonation of the corresponding methylene-bridged complexes, and although the initially targeted tricarbonyl precursor $[RhOs(IMe_4)(CO)_3(\mu\text{-}CH_2)(dppm)_2]^+$ could not be synthesized, the dicarbonyl analogues $[RhOsL(CO)_2(\mu\text{-}CH_2)(dppm)_2][OTf]$ (L = IMe_4 (**9**), PMe_3 (**11**)) were obtained and their protonations by HOTf carried out and compared to that of the carbonyl analogue (L = CO). In all cases (L = CO, PMe_3, IMe_4) the kinetic products, observed at −80 °C, are the unsymmetrically bridged (agostic) methyl species, although for L = PMe_3, IMe_4 minor isomers having terminally bound methyl groups were also observed. In the methyl-bridged products the average C−H coupling constants for these groups decreased in the order L = CO (120 Hz) > PMe_3 (117 Hz) > IMe_4 (111 Hz), consistent with weakening of the agostic C−H bond by increased back-donation as ligand (L) basicity increased. Consistent with our proposal and with Shapley's findings,[11] the bridging methyl products $[RhOsL(CO)_2(\mu\text{-}CH_3)(dppm)_2][OTf]_2$, containing the more basic PMe_3 and IMe_4 ligands, transformed to the respective methylene/hydride tautomers upon warming to ambient temperature. However, this transformation did not occur directly but instead proceeded via an intermediate, $[RhOs(CH_3)(OTf)(L)(CO)_2(dppm)_2][OTf]$ (L = IMe_4 (**14**), PMe_3 (**15**)), having a coordinated triflate ion and the methyl group terminally bound to Os (see Scheme 5). We assume that the dicationic charge of the methyl-bridged species **12a** and **13a** disfavors C−H bond cleavage and that this transformation occurs more readily from a more electron-rich monocationic (presumably also methyl-bridged) species derived from **14** and **15**.

These results do not rule out triflate ion coordination being reversible, with the slower C−H bond cleavage step still occurring from the methyl-bridged species **12a** and **13a**. In order to establish the role of anion coordination in the C−H activation process, we generated $[RhOs(PMe_3)(CO)_2(\mu\text{-}CH_2)(dppm)_2][BPh_4]$ (**11-BPh$_4$**), having a noncoordinating anion, and investigated its protonation by $[H(OEt_2)_2][BAr^F{}_4]$, also having a noncoordinating anion. At −50 °C protonation yields the pair of methyl products analogous to **13a,b**, as obtained with HOTf. However, at this temperature and above these species transform into $[RhOs(CH_3)(PMe_3)(CO)_2(OEt_2)(dppm)_2]^{2+}$ (**18**), containing a terminally bound methyl ligand; no evidence for a methylene/hydride species was obtained in the absence of coordinating anions. This experiment appears to rule out the direct transformation of **13** to **17** and presumably of the analogous IMe_4 species and argues for the intermediacy of a triflate adduct, such as **15**. We have previously observed the conversion of methyl complexes into methylene/hydride products upon ligand addition.[1c,34]

It is interesting that in a previous study the methyl-bridged PMe_3-containing compound $[RhOs(PMe_3)(CO)_3(\mu\text{-}CH_3)(dppm)_2][OTf]_2$,[8a,c] containing an additional carbonyl ligand, did not give rise to the corresponding methylene/hydride tautomer upon warming, as was observed in this study for the dicarbonyl analogue. Presumably, the additional π-accepting carbonyl ligand is enough to disfavor the oxidative addition (methylene/hydride) product.

■ ASSOCIATED CONTENT

Ⓢ Supporting Information. Tables and figures giving crystallographic experimental details for compounds **6**, **8**, and **19b**, NMR spectra for compounds **9** and **11-BPh$_4$**, and spectra and spectral data for the intermediates in the protonation of **11-BPh$_4$** by $[H(OEt_2)_2][BAr^F{}_4]$ and CIF files giving atomic coordinates, interatomic distances and angles, anisotropic thermal parameters, and hydrogen parameters for compounds **6**, **8**, and **19b**. This material is available free of charge via the Internet at http://pubs.acs.org.

■ AUTHOR INFORMATION

Corresponding Author

*E-mail: martin.cowie@ualberta.ca. Fax: 01 7804928231. Tel: 01 7804925581.

■ ACKNOWLEDGMENT

We thank the Natural Sciences and Engineering Research Council of Canada (NSERC) and the University of Alberta for financial support of this research and the NSERC for funding for the Bruker PLATFORM/SMART 1000 CCD diffractometer, and the Nicolet Avatar IR spectrometer. We thank the Department's Analytical and Instrumentation Laboratory and NMR Spectroscopy Laboratory for outstanding support and M. E. Slaney for supplying the sample of $[H(OEt_2)_2][BAr^F{}_4]$.

■ REFERENCES

(1) See for example: (a) Bochmann, M. *J. Organomet. Chem.* **2004**, *689*, 3982. (b) Fukuoka, A.; Sadashima, T.; Endo, I.; Ohashi, N.; Kambara, Y.; Sugiura, T.; Miki, K.; Kasai, N.; Komiya, S. *Organometallics* **1994**, *13*, 4033. (c) Torkelson, J. R.; Antwi-Nsiah, F. H.; McDonald, R.; Cowie, M.; Pruis, J. G.; Jalkanen, K. J.; DeKock, R. L. *J. Am. Chem. Soc.* **1999**, *121*, 3666. (d) Yan, X.; Batchelor, R. J.; Einstein, F. W. B.; Zhang, X.; Nagelkerke, R.; Sutton, D. *Inorg. Chem.* **1997**, *36*, 1237.

(2) See for example: (a) Park, J. W.; Mackenzie, P. B.; Schaefer, W. P.; Grubbs, R. H. *J. Am. Chem. Soc.* **1986**, *108*, 6402. (b) Heinekey, D. M.; Michel, S. T.; Schulte, G. K. *Organometallics* **1989**, *8*, 1241. (c) Dietrich, H. M.; Grove, H.; Törnroos, K. W.; Anwander, R. *J. Am. Chem. Soc.* **2006**, *128*, 1458. (d) Kickham, J. E.; Guérin, F.; Stephan, D. W. *J. Am. Chem. Soc.* **2002**, *124*, 11486.

(3) See for example: (a) Marks, T. J. *Acc. Chem. Res.* **1992**, *25*, 57. (b) Bolton, P. D.; Clot, E.; Cowley, A. R.; Mountford, P. *J. Am. Chem. Soc.* **2006**, *128*, 15005. (c) Bryliakov, K. P.; Talsi, E. P.; Semikolenova, N. V.; Zakharov, V. A. *Organometallics* **2009**, *28*, 3225.

(4) (a) Calvert, R. B.; Shapley, J. R. *J. Am. Chem. Soc.* **1978**, *100*, 7726. (b) Hursthouse, M. B.; Jones, R. A.; Malik, K. M. A.; Wilkinson, G. *J. Am. Chem. Soc.* **1979**, *101*, 4128. (c) Jones, R. A.; Wilkinson, G.; Galas, A. M. R.; Hursthouse, M. B.; Malik, K. M. A. *J. Chem. Soc., Dalton Trans.* **1980**, 1771. (d) Dawkins, G. M.; Green, M.; Orpen, A. G.; Stone, F. G. A. *J. Chem. Soc., Chem. Commun.* **1982**, 41. (e) Casey, C. P.; Fagan, P. J.; Miles, W. H. *J. Am. Chem. Soc.* **1982**, *104*, 1134. (f) Brookhart, M.; Green, M. L. H.; Wong, L.-L. *Prog. Inorg. Chem.* **1988**, *36*, 1 and references therein. (g) Braunstein, P.; Boag, N. M. *Angew. Chem., Int. Ed.* **2001**, *40*, 2427. (h) García, M. E.; Ramos, A.; Ruiz, M. A.; Lanfranchi, M.; Marchio, L. *Organometallics* **2007**, *26*, 6197.

(5) (a) Zaera, F. *Chem. Rev.* **1995**, *95*, 2651. (b) Driessen, M. D.; Grassian, V. H. *J. Am. Chem. Soc.* **1997**, *119*, 1697.

(6) (a) Calvert, R. B.; Shapley, J. R. *J. Am. Chem. Soc.* **1977**, *99*, 5225. (b) Calvert, R. B.; Shapley, J. R.; Schultz, A. J.; Williams, J. M.; Suib, S. L.; Stucky, G. D. *J. Am. Chem. Soc.* **1978**, *100*, 7726. (c) Herrmann, W. A.; Plank, J.; Riedel, D.; Ziegler, M. L.; Weidenhammer, K.; Guggolz, E.; Balbach, B. *J. Am. Chem. Soc.* **1981**, *103*, 63.

(7) (a) Turner, M. L.; Long, H. C.; Shenton, A.; Byers, P. K.; Maitlis, P. M. *Chem. Eur. J.* **1995**, *1*, 549. (b) Maitlis, P. M.; Long, H. C.; Quyoum, R.; Turner, M. L.; Wang, Z.-Q. *Chem. Commun.* **1996**, 1.

(8) For example see: (a) Trepanier, S. J.; McDonald, R.; Cowie, M. *Organometallics* **2003**, *22*, 2638. (b) Rowsell, B. D.; McDonald, R.;

Cowie, M. *Organometallics* **2004**, *23*, 3873. (c) Wigginton, J. R.; Trepanier, S. J.; McDonald, R.; Ferguson, M. J.; Cowie, M. *Organometallics* **2005**, *24*, 6194. (d) Samant, R. G.; Trepanier, S. J.; Wigginton, J. R.; Xu, L.; Bierenstiel, M.; McDonald, R.; Ferguson, M. J.; Cowie, M. *Organometallics* **2009**, *28*, 3407.

(9) (a) Davies, D. L.; Gracey, B. P.; Guerchais, V.; Knox, S. A. R.; Orpen, A. G. *J. Chem. Soc., Chem. Commun.* **1984**, 841. (b) Jeffery, J. C.; Orpen, A. G.; Stone, F. G. A.; Went, M. J. *J. Chem. Soc., Dalton Trans.* **1986**, 173. (c) Gao, Y.; Jennings, M. C.; Puddephatt, R. J. *Organometallics* **2001**, *20*, 1882.

(10) (a) Bursten, B. E.; Cayton, R. H. *J. Am. Chem. Soc.* **1987**, *109*, 6053. (b) Bursten, B. E.; Cayton, R. H. *Organometallics* **1986**, *5*, 1051.

(11) Hamilton, D. H.; Shapley, J. R. *Organometallics* **2000**, *19*, 761.

(12) For examples see: (a) Cavallo, L.; Correa, A.; Costabile, C.; Jacobsen, H. *J. Organomet. Chem.* **2005**, *690*, 5407. (b) Dorta, R.; Stevens, E. D.; Scott, N. M.; Costabile, C.; Cavallo, L.; Hoff, C. D.; Nolan, S. P. *J. Am. Chem. Soc.* **2005**, *127*, 2485. (c) Jacobsen, H.; Correa, A.; Poater, A.; Costabile, C.; Cavallo, L. *Coord. Chem. Rev.* **2009**, *253*, 687. (d) Crabtree, R. H. *J. Organomet. Chem.* **2005**, *690*, 5451.

(13) (a) For examples see: Grubbs, R. H. *Tetrahedron* **2004**, *60*, 7117. (b) Sanford, M. S.; Love, J. A.; Grubbs, R. H. *J. Am. Chem. Soc.* **2001**, *123*, 6543. (c) Sanford, M. S.; Ulman, M.; Grubbs, R. H. *J. Am. Chem. Soc.* **2001**, *123*, 749. (d) Dröge, T.; Glorius, F. *Angew. Chem., Int. Ed.* **2010**, *49*, 6940. (e) Lee, M.-T.; Lee, H. M.; Hu, C.-H. *Organometallics* **2007**, *26*, 1317.

(14) Kuhn, N.; Kratz, T. *Synthesis* **1993**, *6*, 561.

(15) Hilts, R. W.; Franchuk, R. A.; Cowie, M. *Organometallics* **1991**, *10*, 304.

(16) Trepanier, S. J.; Dennett, J. N. L.; Sterenberg, B. T.; McDonald, R.; Cowie, M. *J. Am. Chem. Soc.* **2004**, *126*, 8046.

(17) Brookhart, M.; Grant, B.; Volpe, A. F., Jr. *Organometallics* **1992**, *11*, 3920.

(18) Programs for diffractometer operation, unit cell indexing, data collection, data reduction, and absorption correction were those supplied by Bruker.

(19) Sheldrick, G. M. *Acta Crystallogr.* **2008**, *A64*, 112.

(20) Altomare, A.; Burla, M. C.; Camalli, M.; Cascarano, G. L.; Giacovazzo, C.; Guagliardi, A.; Moliterni, A. G. G.; Polidori, G.; Spagna, R. *J. Appl. Crystallogr.* **1999**, *32*, 115.

(21) van der Sluis, P.; Spek, A. L. *Acta Crystallogr.* **1990**, *A46*, 194–201.

(22) Spek, A. L. *Acta Crystallogr.* **1990**, *A46*, C34.*PLATON-a Multipurpose Crystallographic tool*; Utrecht University, Utrecht, The Netherlands, 1990.

(23) (a) Herrmann, W. A.; Elison, M.; Fischer, J.; Köcher, C.; Artus, G. R. J. *Chem. Eur. J.* **1996**, *2*, 772. (b) Bortenschlager, M.; Schütz, J.; von Preysing, D.; Nuyken, O.; Herrmann, W. A.; Weberskirch, R. *J. Organomet. Chem.* **2005**, *690*, 6233.

(24) Wells, K. D.; Ferguson, M. J.; McDonald, R.; Cowie, M. *Organometallics* **2008**, *27*, 691.

(25) For examples see: (a) Torkelson, J. R.; Oke, O.; Muritu, J.; McDonald, R.; Cowie, M. *Organometallics* **2000**, *19*, 854. (b) Sterenberg, B. T.; Hilts, R. W.; Moro, G.; McDonald, R.; Cowie, M. *J. Am. Chem. Soc.* **1995**, *117*, 245. (c) Wells, K. D.; Ferguson, M. J.; McDonald, R.; Cowie, M. *Organometallics* **2011**, *30*, 815.(d) Wells, K. D.; McDonald, R.; Ferguson, M. J.; Cowie, M. *Inorg. Chem.* **2011**, *50*, 3523 (e) Dawkins, G. M.; Green, M.; Jeffery, J. C.; Sambale, C.; Stone, F. G. A. *J. Chem. Soc., Dalton Trans.* **1983**, 499. (f) Brown, M. P.; Yavari, A.; Manojlovic-Muir, L.; Muir, K. W. *J. Organomet. Chem.* **1983**, *256*, C19. (g) Sharp, P. R.; Ge, Y. W. *J. Am. Chem. Soc.* **1987**, *109*, 3796. (h) Ge, Y. W.; Sharp, P. R. *Organometallics* **1988**, *7*, 2234. (i) Ge, Y. W.; Peng, F.; Sharp, P. R. *J. Am. Chem. Soc.* **1990**, *112*, 2632. (j) Ge, Y. W.; Sharp, P. R. *Inorg. Chem.* **1992**, *31*, 379. (k) Ye, C.; Sharp, P. R. *Inorg. Chem.* **1995**, *34*, 55.

(26) (a) Kim, Y.-J.; Streitwieser, A. *J. Am. Chem. Soc.* **2002**, *124*, 5757. (b) Magill, A. M.; Cavell, K. J.; Yates, B. F. *J. Am. Chem. Soc.* **2004**, *126*, 8717. (c) Alder, R. W.; Allen, P. R.; Williams, S. J. *Chem. Commun.* **1995**, 1267. (d) Hui Deng, Y. C; Cheng, J.-P. *J. Org. Chem.* **2007**, *72*, 7790.

(27) Marat, K. *SpinWorks V*; University of Manitoba.

(28) (a) Green, M. L. H.; Hughes, A. K.; Popham, N. A.; Stephens, A. H. H.; Wong, L.-L. *J. Chem. Soc., Dalton Trans.* **1992**, 3077. (b) Saunders, M.; Jaffe, M. H.; Vogel, P. *J. Am. Chem. Soc.* **1971**, *93*, 2558.

(29) Lambert, J. B.; Greifenstein, L. G. *J. Am. Chem. Soc.* **1974**, *96*, 5120.

(30) Grossmann, G.; Lang, R.; Ohms, G.; Scheller, D. *Magn. Reson. Chem.* **1990**, *28*, 500.

(31) (a) Oke, O.; McDonald, R.; Cowie, M. *Organometallics* **1999**, *18*, 1629. (b) Dell'Anna, M. M.; Trepanier, S. J.; McDonald, R.; Cowie, M. *Organometallics* **2001**, *20*, 88. (c) Rowsell, B. D.; Trepanier, S. J.; Lam, R.; McDonald, R.; Cowie, M. *Organometallics* **2002**, *21*, 3228.

(32) (a) Arduengo, A. J.; Calabrese, J. C.; Davidson, F.; Dias, H. V. R.; Goerlich, J. R.; Krafczyk, R.; Marshall, W. J.; Tamm, M.; Schmutzler, R. *Helv. Chim. Acta* **2009**, *92*, 2348. (b) Edwards, P. G.; Hahn, F. E.; Limon, M.; Newman, P. D.; Kariuki, B. M.; Stasch, A. A. *Dalton Trans.* **2009**, 5115.

(33) (a) McGuinness, D. S.; Cavell, K. J.; Skelton, B. W.; White, A. H. *Organometallics* **1999**, *18*, 1596. (b) Martin, H. C.; James, N. H.; Aitken, J.; Gaunt, J. A.; Adams, H.; Haynes, A. *Organometallics* **2003**, *22*, 4451. (c) McGuinness, D. S.; Saendig, N.; Yates, B. F.; Cavell, K. J. *J. Am. Chem. Soc.* **2001**, *123*, 4029. (d) McGuinness, D. S.; Cavell, K. J. *Organometallics* **2000**, *19*, 4918.

(34) (a) Ristic-Petrovic, D.; Anderson, D. J.; Torkelson, J. R.; McDonald, R.; Cowie, M. *Organometallics* **2003**, *22*, 4647. (b) Ristic-Petrovic, D.; Anderson, D. J.; Torkelson, J. R.; Ferguson, M. J.; McDonald, R.; Cowie, M. *Organometallics* **2005**, *24*, 3711. (c) Slaney, M. E.; Anderson, D. J.; McDonald, R.; Ferguson, M. J.; Cowie, M. *J. Am. Chem. Soc.* **2010**, *132*, 16544.